ISSN 1949-8470 (online)

World Journal of *Radiology*

World J Radiol 2024 March 28; 16(3): 40-71

Published by Baishideng Publishing Group Inc

World Journal of Radiology

Contents

Monthly Volume 16 Number 3 March 28, 2024

World Journal of Radiology

Monthly Volume 16 Number 3 March 28, 2024

Contents

ABOUT COVER

Editorial Board Member of *World Journal of Radiology*, Bilgin Kadri Aribas, MD, Professor, Department of Radiology, Department of Radiology, Bülent Ecevit Üniversitesi Tıp Fakültesi Radyoloji AnaBilim Dalı Zonguldak, Zonguldak 67600, Turkey. bilginaribas@hotmail.com

AIMS AND SCOPE

The primary aim of *World Journal of Radiology* (*WJR*, *World J Radiol*) is to provide scholars and readers from various fields of radiology with a platform to publish high-quality basic and clinical research articles and communicate their research findings online.

WJR mainly publishes articles reporting research results and findings obtained in the field of radiology and covering a wide range of topics including state of the art information on cardiopulmonary imaging, gastrointestinal imaging, genitourinary imaging, musculoskeletal imaging, neuroradiology/head and neck imaging, nuclear medicine and molecular imaging, pediatric imaging, vascular and interventional radiology, and women's imaging.

INDEXING/ABSTRACTING

The *WJR* is now abstracted and indexed in PubMed, PubMed Central, Emerging Sources Citation Index (Web of Science), Reference Citation Analysis, China Science and Technology Journal Database, and Superstar Journals Database. The 2023 Edition of Journal Citation Reports® cites the 2022 impact factor (IF) for *WJR* as 2.5; IF without journal self cites: 2.3; 5-year IF: 2.5; Journal Citation Indicator: 0.54.

RESPONSIBLE EDITORS FOR THIS ISSUE

Production Editor: *Si Zhao*; **Production Department Director:** *Xu Guo*; **Cover Editor:** *Jia-Ping Yan*.

NAME OF JOURNAL
World Journal of Radiology

ISSN
ISSN 1949-8470 (online)

LAUNCH DATE
January 31, 2009

FREQUENCY
Monthly

EDITORS-IN-CHIEF
Thomas J Vogl

EDITORIAL BOARD MEMBERS
https://www.wjgnet.com/1949-8470/editorialboard.htm

PUBLICATION DATE
March 28, 2024

COPYRIGHT
© 2024 Baishideng Publishing Group Inc

INSTRUCTIONS TO AUTHORS
https://www.wjgnet.com/bpg/gerinfo/204

GUIDELINES FOR ETHICS DOCUMENTS
https://www.wjgnet.com/bpg/GerInfo/287

GUIDELINES FOR NON-NATIVE SPEAKERS OF ENGLISH
https://www.wjgnet.com/bpg/gerinfo/240

PUBLICATION ETHICS
https://www.wjgnet.com/bpg/GerInfo/288

PUBLICATION MISCONDUCT
https://www.wjgnet.com/bpg/gerinfo/208

ARTICLE PROCESSING CHARGE
https://www.wjgnet.com/bpg/gerinfo/242

STEPS FOR SUBMITTING MANUSCRIPTS
https://www.wjgnet.com/bpg/GerInfo/239

ONLINE SUBMISSION
https://www.f6publishing.com

© 2024 Baishideng Publishing Group Inc. All rights reserved. 7041 Koll Center Parkway, Suite 160, Pleasanton, CA 94566, USA
E-mail: office@baishideng.com https://www.wjgnet.com

World Journal of Radiology

Submit a Manuscript: https://www.f6publishing.com

World J Radiol 2024 March 28; 16(3): 40-48

DOI: 10.4329/wjr.v16.i3.40

ISSN 1949-8470 (online)

MINIREVIEWS

Chronic pancreatitis: Pain and computed tomography/magnetic resonance imaging findings

Yue Feng, Ling-Ji Song, Bo Xiao

Specialty type: Radiology, nuclear medicine and medical imaging

Provenance and peer review: Invited article; Externally peer reviewed.

Peer-review model: Single blind

Peer-review report's scientific quality classification

Grade A (Excellent): 0
Grade B (Very good): 0
Grade C (Good): C
Grade D (Fair): 0
Grade E (Poor): 0

P-Reviewer: Machado MC, Brazil

Received: December 27, 2023
Peer-review started: December 27, 2023
First decision: January 5, 2024
Revised: January 19, 2024
Accepted: February 26, 2024
Article in press: February 26, 2024
Published online: March 28, 2024

Yue Feng, Ling-Ji Song, Department of Radiology, The Affiliated Hospital of North Sichuan Medical College, Nanchong 637000, Sichuan Province, China

Bo Xiao, Department of Radiology, Bishan Hospital of Chongqing Medical University, Bishan Hospital of Chongqing, Chongqing 402760, China

Corresponding author: Bo Xiao, MD, PhD, Associate Professor, Director, Doctor, Teacher, Department of Radiology, Bishan Hospital of Chongqing Medical University, Bishan Hospital of Chongqing, No. 9 Shuangxing Da Road, Chongqing 402760, China.
xiaoboimaging@163.com

Abstract

Chronic pancreatitis (CP) is a fibroinflammatory disease characterized by irreversible destruction of pancreatic tissue. With the development of the disease, it may lead to exocrine and/or endocrine insufficiency. CP is one of the common diseases that cause abdominal pain, which will not get permanent spontaneous relief as the disease evolves. The American College of Gastroenterology clinical guidelines recommend computed tomography or magnetic resonance imaging as the first-line examination for the diagnosis of CP. CP common imaging findings include pancreatic atrophy, irregular dilatation of the pancreatic duct, calcification of pancreatic parenchyma, pancreatic duct stones, *etc.* In clinical practice, whether any correlations between CP-induced abdominal pain patterns (no pain/constant/intermittent pain) and corresponding imaging findings present are not well known. Therefore, this review aims to comprehensively sort out and analyze the relevant information by collecting lots of literature on this field, so as to construct a cross-bridge between the clinical manifestations and imaging manifestations of CP patients. Also, it provides an imaging basis and foundation for the classification and diagnosis of abdominal pain types in clinical CP patients.

Key Words: Chronic pancreatitis; Pancreatitis; Abdominal pain; Computed tomography; Magnetic resonance imaging

©The Author(s) 2024. Published by Baishideng Publishing Group Inc. All rights reserved.

Core Tip: Chronic pancreatitis (CP) is a fibroinflammatory syndrome. On the one hand, pain is the most common clinical manifestation of CP. On the other hand, computed tomography (CT)/magnetic resonance imaging (MRI) is the most commonly used imaging examination for CP, and the American College of Gastroenterology clinical guidelines recommend CT or MRI as the first-line examination for the diagnosis of CP. However, there is no review on whether there is a correlation between pain and CT/MRI. For this reason, this article focuses on summarizing the relationship between the pain patterns or types of the CP and the corresponding CT/MRI imaging findings, which is conducive to the integration of relevant and scattered contents, and is conducive to building a cross-bridge between clinical manifestations and imaging findings of CP patient. At the same time, it will promote academic exchanges between different medical centers as well as scientific research and teaching.

Citation: Feng Y, Song LJ, Xiao B. Chronic pancreatitis: Pain and computed tomography/magnetic resonance imaging findings. *World J Radiol* 2024; 16(3): 40-48
URL: https://www.wjgnet.com/1949-8470/full/v16/i3/40.htm
DOI: https://dx.doi.org/10.4329/wjr.v16.i3.40

INTRODUCTION

Chronic pancreatitis (CP) is a fibroinflammatory syndrome caused by various causes. Long-term recurrent pancreatitis causes normal pancreatic parenchyma to be replaced by fibrotic tissues. With the development of the disease, pancreatic tissue and function undergo irreversible changes and destruction, which eventually lead to chronic abdominal pain, exocrine and endocrine pancreatic insufficiency[1,2].

The global incidence of CP is approximately 10 cases per 100,000 general population per year, and the incidence is increasing over time. Notably, the incidence of CP is twice as high in men as in women[3,4]. The general clinical manifestations of patients with CP are abdominal pain, nausea, vomiting, *etc.*, among which abdominal pain is the most common (about 76% of CP patients)[5]. However, although it is not common, 10% of patients with CP are pain-free[6]. The pain manifestations of CP are highly variable and diverse, which can even be converted to each other. Unfortunately, the mechanism of pain is incompletely understood.

For the diagnosis of CP, the American College of Gastroenterology (ACG) clinical guidelines recommend computed tomography (CT) or magnetic resonance imaging (MRI) as the first-line examination[7].

The objective of the present review is to deeply investigate the pain, CT or MRI manifestations of CP patients, and to find out whether there are some change trends or relationships between pain and imaging findings, so as to build a cross-bridge between clinical manifestations and imaging manifestations of CP patients. Also, it can provide an imaging basis and foundation for the classification and diagnosis of abdominal pain types in clinical CP patients, which may improve the diagnostic accuracy and the prognosis of CP patients.

PRELIMINARY UNDERSTANDING OF CP

The first definition of CP was proposed in 1946[8], and a new mechanistically derived definition of CP was published by Whitcomb *et al*[9] in 2016, that is, CP is characterized by pathologic fibro-inflammatory syndrome of the pancreas in individuals with genetic, environmental and other risk factors such as hypercalcemia, hypertriglyceridemia, autoimmune disorders and so forth. Advanced CP is featured with pancreatic atrophy, fibrosis, chronic pain, ductal distortion and strictures, calcifications, dysplasia, pancreatic exocrine dysfunction, and endocrine dysfunction[9,10].

CP is a fibroinflammatory disease of the pancreas. Its pathophysiology is very complex and the pathogenesis is not completely understood. Although the mechanism of CP is complex, a large number of studies have shown a similar development trend, that is, various causes lead to progressive irreversible damage to the pancreatic parenchyma, and the pancreatic enzymes release following the injury of the exocrine tissue leading to inflammation. Long-term recurrent pancreatitis and injury can activate pancreatic stellate cells, leading to the formation of fibers and scars. Finally, the pancreas shrinks and hardens, resulting in exocrine and endocrine insufficiency of the pancreas[11-14].

THE PAIN OF CP

The clinical manifestations of CP are mainly upper abdominal pain, which is complex and multimodal. The pain pattern varies according to the temporal nature and severity of CP. According to the temporal nature of pain, it can be divided into constant or intermittent pain[15]. According to the severity of pain, it can be divided into mild, moderate, or severe. Previous studies[10,16,17] used five types of pain patterns (A-E) (Table 1), and patients were required to choose from five pain patterns according to the type and severity of their pain. The most common pain pattern is the 'D' type, which is characterized by constant mild to moderate pain plus episodes of severe pain. In addition, in a retrospective study of 54 CP patients, Bahuva *et al*[18] found that the presence or absence of pain was not significantly related to the severity of CP

Table 1 Patterns and classification of pain[10,16,17]

Pattern	Implication
A	Usually, pain-free with episodes of mild to moderate pain
B	Constant mild to moderate pain
C	Usually, pain-free with episodes of severe pain
D	Constant mild to moderate pain plus episodes of severe pain
E	Constant severe pain
Frequency of pain	
Intermittent	Pain pattern A or C
Constant	Pain pattern B, D or E
Severity of pain	
Mild-moderate	Pain pattern A or B
Severe	Pain pattern C, D or E

structural changes, regardless of the structural changes. Therefore, this study showed that pancreatic morphological abnormalities had a poor predictive ability for CP pain.

CP not only have a variety of pain patterns but also have a complex mechanism of pain. Including multiple factors, such as pancreatitis; the pancreatic duct is compressed and narrowed due to stones or strictures, which may lead to duct hypertension or pancreatic ischemia and further cause pain; and complications such as pseudocysts, local inflammatory masses, duodenal and bile duct obstruction[19,20]. At present, the common CP pain assessment tools recommended by the international consensus guidelines include the Visual Analogue scale, Izbiki pain score, McGill Pain Questionnaire, and so on[21].

In the early years, some scholars[22,23] believed that the spontaneous relief of pain depended on the progressive development of CP, and believed that the pain of CP would improve with progressive pancreatic insufficiency (such as severe exocrine/endocrine insufficiency, severe duct abnormalities, more pancreatic calcification, *etc.*), especially for alcoholic CP, which is the so-called "burn-out" hypothesis.

However, most studies[16,24,25] have shown that the pain of CP did not seem to be significantly improved over time, and it was not uncommon for patients to experience pain recurrence during follow-up.

Combined with the study of Dimcevski *et al*[26], it has been shown that there are neurological components in CP-induced pain, and cortical reorganization is a pathogenesis of CP patients, indicating that the pain of CP may be largely independent of pancreatic fibrosis and progressive pancreatic insufficiency. The possible phenomenon is that as the disease progresses, the pain of CP patients may be alleviated, but it cannot be significantly relieved permanently. Therefore, waiting for spontaneous pain relief seems to be inaccurate and not worthy of praise.

CT/MRI FINDINGS OF CP

The diagnosis of CP is to combine its clinical features with characteristics of CT or MRI, endoscopic ultrasonography (EUS), and pancreatic function examination[7,19]. Clinically, CT or MRI recommended by the ACG clinical guidelines are often used as the first-line examination for the diagnosis of CP[7]. The diagnostic criteria for CP can be traced back to the Cambridge classification of pancreatic morphology in 1984 (Table 2)[27], and the M-Annheim classification of CP proposed by Schneider *et al*[14] in 2007 (Table 3), as detailed in the tables.

The progression of CP can be divided into early and advanced stages. The early stage especially refers to the period before the development of morphological changes in the pancreas. Because the morphology of the pancreas is mostly normal at this time, it is difficult to diagnose by conventional imaging methods. In the advanced stage, the morphology of the pancreas changes, which often manifests as pancreatic atrophy, pancreatic parenchyma calcification, irregular dilatation and distortion of the pancreatic duct, intraductal calculi, *etc.*, and it can also be accompanied by complications, such as pseudocyst, common bile duct stricture, duodenal obstruction, *etc.* These manifestations can be detected by conventional radiological imaging (CT or MRI)[28]. CT scan is easily available, noninvasive, and relatively cheaper compared to other modalities. MRI is superior to CT for the evaluation of pancreatic parenchymal and ductal changes, with better resolution than CT, but it is more expensive and requires more time.

Three common CT findings of CP are pancreatic ductal dilatation (68%; Figure 1A), parenchymal atrophy (54%; Figure 1B), and pancreatic calcification (50%; Figure 1B)[19]. MRI shows pancreatic duct stones better than CT, while CT shows calcification better than MRI.

In recent years, most of the literature and guidelines[29,30] emphasize the importance of early diagnosis of CP, and achieve the purpose of early detection and early diagnosis before irreversible changes in the pancreas, so as to avoid late complications and improve the prognosis and clinical outcomes of CP patients.

Table 2 Cambridge classification diagnostic criteria in chronic pancreatitis[27]

To evaluate chronic pancreatitis from the aspects of pancreatic parenchyma, pancreatic duct morphology, local changes, and so on by CT and US		
Normal	Quality study visualising the whole gland without abnormal features	
Equivocal	One sign only	Main duct enlarged (< 4 mm)
		Gland enlarged (up to 2 × normal)
		Cavities (< 10 mm)
		Irregular ducts
		Focal acute pancreatitis
		Parenchymal heterogeneity
Mild changes	Two or more signs	Duct wall echoes increased
Moderate changes		Irregular head/body contour
Marked changes	As above, and with one or more of: Large cavities (> 10 mm), gross gland enlargement (> 2 × normal), intraductal filling defects or calculi, duct obstruction, structure or gross irregularity, contiguous organ invasion	

CT: Computed tomography; US: Ultrasound.

Table 3 M-Annheim diagnostic criteria of definite chronic pancreatitis[14]

At least one of the following four items should be met
Pancreatic calcifications
Moderate or marked ductal lesions (according to the Cambridge classification)
Marked and persistent exocrine insufficiency defined as pancreatic steatorrhea markedly reduced by enzyme supplementation
Typical histology of an adequate histological specimen

Early diagnosis of pancreatic fibrosis can provide a valuable opportunity to prevent disease progression[11]. Khatkov *et al*[11] believed that multidetector CT (MDCT) can be used as a non-invasive diagnostic tool for detecting pancreatic fibrosis, and its post-processing indicators are related to the degree of pancreatic fibrosis, so it is expected to be used for early diagnosis of CP. The results of a study involving 74 patients showed that compared with mild pancreatic fibrosis, the normalized contrast enhancement ratio during the venous phases and the pancreatic late/early attenuation ratio increased in patients with severe pancreatic fibrosis, while the unenhanced pancreatic density decreased. Therefore, the application value of MDCT in the early diagnosis of CP is further verified.

A prospective study by Liu *et al*[31] showed that pancreatic stiffness and T1 relaxation time in multimodal functional MRI can be used as independent predictors of pancreatic fibrosis grading and showed significant associations with fibrosis extent. And substantial changes in mild CP can be detected by T1-mapping, which is manifested by a significant increase in the T1 relaxation time of pancreatic parenchyma in patients with mild CP[32]. Therefore, T1-mapping can also be used as a new MRI technique to evaluate early CP. In addition, magnetic resonance elastography (MRE)-derived stiffness, which can be used to measure tissue mechanical properties and provide information on soft tissue stiffness in vivo, is the highest diagnostic indicator for detecting CP without secretory insufficiency (reflecting early CP), and there is no difference in the diagnostic effect between T1 relaxation time and MRE-derived stiffness[28]. Furthermore, the research of Wang *et al*[33] showed that multitasking dynamic contrast enhanced MRI technology can not only achieve early detection and early diagnosis of CP because changes in microcirculation characteristics are usually preceded by morphological changes, but also it can identify and diagnose CP and pancreatic ductal adenocarcinoma by estimating microcirculation parameters (such as tissue plasma flow, fractional plasma volume, transfer constant, *etc*.).

THE RELATIONSHIP BETWEEN PAIN AND IMAGING FINDINGS OF CP

Before this, there were many studies on the correlation between the pain of CP and its imaging morphological manifestations, but they were scattered and not concentrated. On one hand, pain is the most common clinical manifestation of CP. On the other hand, CT/MRI is the most commonly used imaging examination for CP. There is no review to summarize the correlation and connection between the two. Here, it is summarized in the form of tables (Table 4) and text, in order to find something valuable.

Table 4 The relationship between pain and imaging findings of chronic pancreatitis

Ref.	*n*	Research type	Imaging techniques	Results
Bornman *et al* [34], 1980	47	A prospective study	ERCP	The incidence of pancreatic duct obstruction or stricture in patients with painless and painful CP was comparable, indicating that the morphological changes of the pancreatic duct are not related to the occurrence of pain
Jensen *et al*[35], 1984	101	A comparative study	ERP	There was no correlation between the degree of pain in CP (no pain, light pain, moderate pain, severe pain) and the dilatation of the main pancreatic duct measured by ERP (the diameter of the main pancreatic duct in the pancreatic body exceeding 5 mm was defined as dilatation)
Malfertheiner *et al* [37], 1987	64	A prospective study	CT/ERP	There was a poor correlation between the severity of pain and abdominal imaging features in CP patients, but it was also found that patients with large pancreatic cysts were most often associated with severe pain (62%), while enlargement of pancreatic gland, small cysts, and duct dilatation were roughly the same as different degrees of pain. Most (89%) patients with calcification still had pain and some of them (39%) showed severe pain
Morgan *et al* [36], 2003	25	A retrospective study	ERCP	There was a poor correlation between the morphological changes of the main pancreatic duct (whether the duct was dilated or blocked) and pain
Mullady *et al* [16], 2011	414	A prospective cohort study	CT/ERCP	The duration of disease in CP patients was not related to either the frequency of pain (intermittent *vs* constant) or the severity of pain (mild, moderate or severe)
Bahuva *et al* [18], 2013	54	A retrospective study	CT/MRCP/EUS	The presence or absence of visceral pain is not significantly related to the severity of CP structural changes, whether the structural changes are severe, mild, or absent
Frøkjær *et al* [39], 2013	40	A controlled study	MRCP/DWI	The pancreatic pathological imaging findings of the fibrotic changes as well as atrophy and ductal pathology were not associated with pain
Wilcox *et al* [17], 2015	518	A retrospective study	CT/MRI/MRCP/EUS/ERCP	CP patients with different pain patterns, temporal nature of pain (no pain, intermittent, constant) or pain severity (no pain, mild-moderate, severe) were very similar in the distribution of imaging findings
Madzak *et al* [2], 2017	82	A prospective cohort study	s-MRI	There was no correlation between pancreatic parenchyma and ductal changes, pain severity, and pain interference scores

CT: Computed tomography; MRCP: Magnetic resonance cholangiopancreatography; EUS: Endoscopic ultrasound; ERP: Endoscopic retrograde pancreatography; ERCP: Endoscopic retrograde cholangio-pancreatography; DWI: Diffusion-weighted imaging; MRI: Magnetic resonance imaging; s-MRI: Secretin-stimulated magnetic resonance imaging; CP: Chronic pancreatitis.

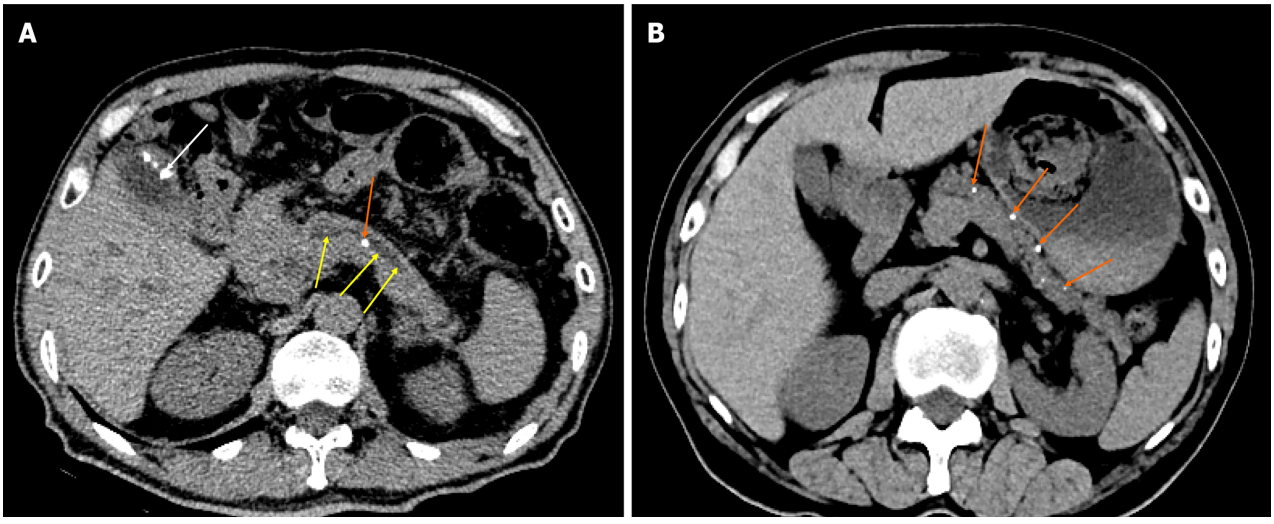

Figure 1 Chronic pancreatitis. A: Chronic pancreatitis with main pancreatic duct stone and main pancreatic duct dilatation. A 58-year-old man with chronic pancreatitis presented with no pain. The abdominal computed tomography (CT) scan represents the main pancreatic duct stone (orange arrow), the dilated main pancreatic duct (yellow arrows) with a diameter of 0.5 cm, as well as the combined gallbladder multiple stones (white arrow); B: Chronic pancreatitis with pancreatic parenchymal atrophy and multiple pancreatic calcifications. A 69-year-old man with chronic pancreatitis. The abdominal CT scan shows a decrease in pancreatic volume, parenchymal atrophy, and multiple calcifications in the pancreatic parenchyma (orange arrows).

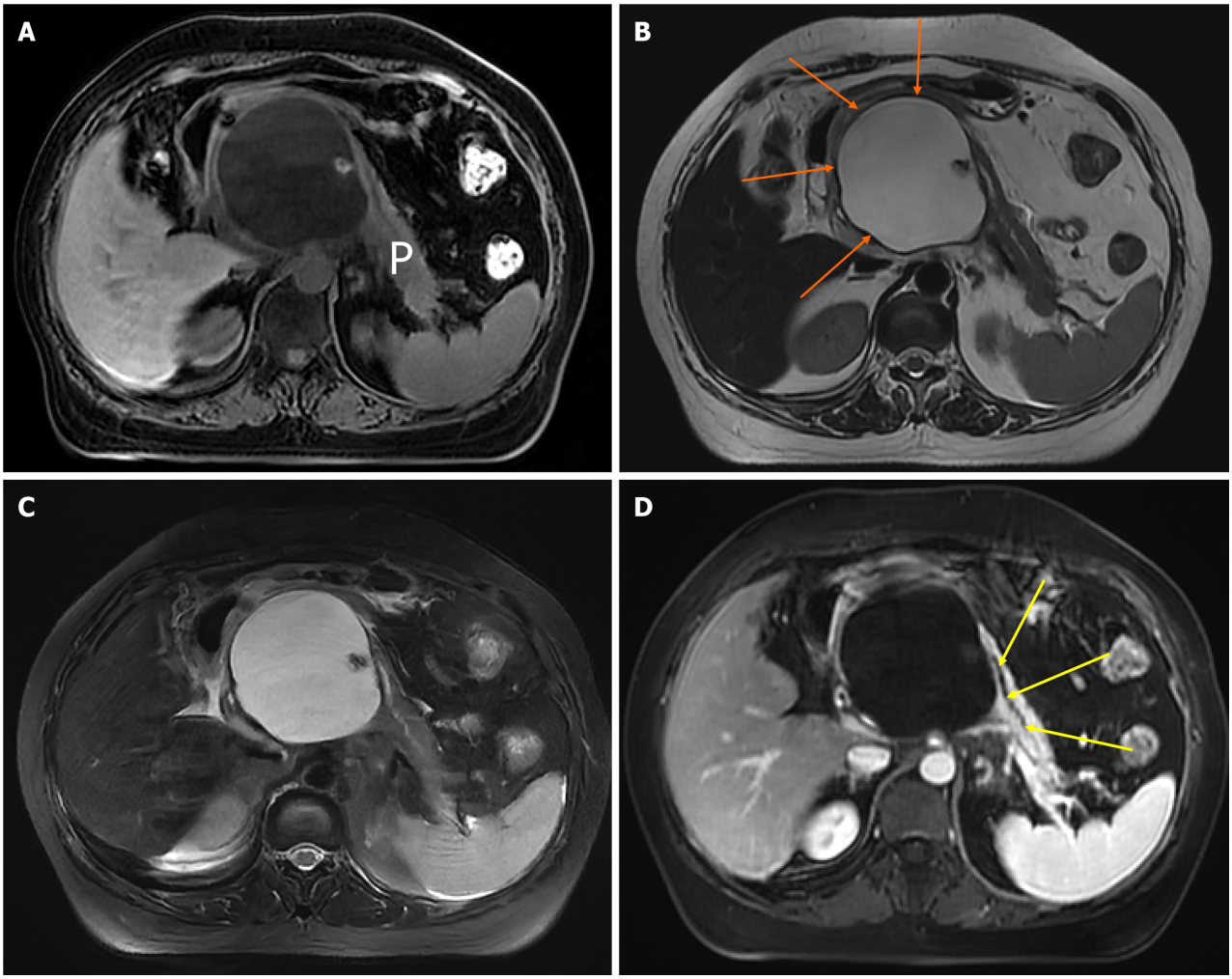

Figure 2 Chronic pancreatitis with large pancreatic cysts. A 52-year-old woman with chronic pancreatitis presented with upper abdominal pain. The upper abdominal magnetic resonance images. A: Magnetic resonance imaging (MRI) fat-suppressed T1-weighted imaging shows a large pseudocyst of the head of the pancreas, which has a low signal; B: MRI T2-weighted imaging can show a clear boundary of pseudocyst (orange arrows) with a diameter of 7 cm × 11 cm, which has a high signal; C: MRI fat-suppressed T2-weighted imaging; D: MRI enhanced scanning venous phase shows the large pseudocyst has no enhancement as well as the displaced main pancreatic duct (yellow arrows). P: Pancreas.

It can be traced back to a study of 47 patients with CP by Bornman *et al*[34] in 1980. The ERCP examination technique used in the study showed that the incidence of pancreatic duct obstruction or stricture was comparable between painless and painful CP patients, indicating that the morphological changes of the pancreatic duct were not related to the occurrence of pain. Along this line, it can be found in subsequent studies that Jensen *et al*[35] found there was no correlation between the expansion of the main pancreatic duct and the severity of pain in patients with CP in a comparative study of 101 patients. Similarly, Morgan *et al*[36] also confirmed that in patients with CP, whether the main pancreatic duct was dilated or blocked, the pain performance was similar. Therefore, it is not hard to see that there is no significant correlation between the presence or severity of pain in CP patients and the morphological changes (dilatation or stricture) of the pancreatic duct.

In addition, further studies[18] also found that there was no significant correlation between the presence or absence of abdominal pain and the severity of CP morphological structural changes. A retrospective study of 518 CP patients was conducted by Wilcox *et al*[17] using CT/MRI/MRCP and other imaging methods. It was found that CP patients with different pain patterns, temporal nature of pain (no pain, intermittent, constant), or severity of pain (no pain, mild-moderate, severe) were very similar in the distribution of imaging findings.

In summary, the severity and duration of abdominal pain symptoms caused by CP are not significantly correlated with the degree of damage to pancreatic anatomical structures (such as pancreatic parenchymal atrophy, pancreatic duct dilatation or stricture, and pancreatic parenchymal fibrosis). However, although the correlation between pain and imaging morphological changes is poor, some other meaningful things have been found. For example, CP patients with large pancreatic cysts are most often associated with severe pain (Figure 2) The correlation between pancreatic enlargement, small cysts duct dilatation, and different degrees of pain is roughly the same. Furthermore, the vast majority of patients with calcification still have pain, and some of them can be manifested as severe pain[37].

Moreover, it was found that the duration of disease in CP patients was not related to either the frequency of pain (intermittent *vs* constant) or the severity of pain (mild, moderate, or severe)[16]. Combined with CP-induced pancreatic neural alterations, such as intrapancreatic nerves increase in size (neural hypertrophy) and number (increased neural

density), related studies have shown that these neural alterations are related to the severity of neuropathic pain. Therefore, the neural alterations of CP are active shapers of disease evolution and progression[38]. This means that a series of pancreatic morphological imaging findings (such as parenchymal atrophy and pancreatic duct dilatation) with the progression of CP may not be related to the severity of pain in patients, and the presence or absence of visceral pain has nothing to do with the severity of CP because most of the pain drivers of advanced CP are neurological rather than pancreatic. Therefore, it is not difficult to explain why the correlation between pain symptoms and imaging findings is poor[18,39].

CONCLUSION

In summary, CP is a fibroinflammatory syndrome caused by a variety of causes. The most common clinical manifestation is abdominal pain and the mechanism of abdominal pain is not fully understood. CT/MRI is usually used as the first-line imaging diagnosis of CP. The duration and severity of abdominal pain caused by CP are poorly correlated with pancreatic imaging morphological changes. There is a correlation between pain caused by CP and neural alterations and related complications. Therefore, the next research should further explore the relationship between neural alterations or related complications caused by CP and pain, in order to have a deeper understanding of CP.

FOOTNOTES

Author contributions: Feng Y, Song LJ and Xiao B designed the research study; Feng Y, Song LJ and Xiao B analyzed the data and wrote the manuscript; All authors have read and approved the final manuscript.

Conflict-of-interest statement: All the authors report no relevant conflicts of interest for this article.

Open-Access: This article is an open-access article that was selected by an in-house editor and fully peer-reviewed by external reviewers. It is distributed in accordance with the Creative Commons Attribution NonCommercial (CC BY-NC 4.0) license, which permits others to distribute, remix, adapt, build upon this work non-commercially, and license their derivative works on different terms, provided the original work is properly cited and the use is non-commercial. See: https://creativecommons.org/Licenses/by-nc/4.0/

Country/Territory of origin: China

ORCID number: Ling-Ji Song 0000-0003-4508-9654; Bo Xiao 0000-0001-5862-974X.

S-Editor: Li L
L-Editor: A
P-Editor: Zhao S

REFERENCES

1 **Beyer G**, Habtezion A, Werner J, Lerch MM, Mayerle J. Chronic pancreatitis. *Lancet* 2020; **396**: 499-512 [PMID: 32798493 DOI: 10.1016/S0140-6736(20)31318-0]
2 **Madzak A**, Olesen SS, Lykke Poulsen J, Bolvig Mark E, Mohr Drewes A, Frøkjær JB. MRI assessed pancreatic morphology and exocrine function are associated with disease burden in chronic pancreatitis. *Eur J Gastroenterol Hepatol* 2017; **29**: 1269-1275 [PMID: 28857897 DOI: 10.1097/MEG.0000000000000955]
3 **Xiao AY**, Tan ML, Wu LM, Asrani VM, Windsor JA, Yadav D, Petrov MS. Global incidence and mortality of pancreatic diseases: a systematic review, meta-analysis, and meta-regression of population-based cohort studies. *Lancet Gastroenterol Hepatol* 2016; **1**: 45-55 [PMID: 28404111 DOI: 10.1016/S2468-1253(16)30004-8]
4 **Petrov MS**, Yadav D. Global epidemiology and holistic prevention of pancreatitis. *Nat Rev Gastroenterol Hepatol* 2019; **16**: 175-184 [PMID: 30482911 DOI: 10.1038/s41575-018-0087-5]
5 **Thompson BS**, Philcox S, Devereaux B, Metz AJ, Croagh D, Gray A, Hamarneh Z, Windsor JA, Neale RE. Prodromal Signs and Symptoms of Chronic Pancreatitis: A Systematic Review. *J Clin Gastroenterol* 2022; **56**: e1-e10 [PMID: 34049375 DOI: 10.1097/MCG.0000000000001544]
6 **Cohen SM**, Kent TS. Etiology, Diagnosis, and Modern Management of Chronic Pancreatitis: A Systematic Review. *JAMA Surg* 2023; **158**: 652-661 [PMID: 37074693 DOI: 10.1001/jamasurg.2023.0367]
7 **Gardner TB**, Adler DG, Forsmark CE, Sauer BG, Taylor JR, Whitcomb DC. ACG Clinical Guideline: Chronic Pancreatitis. *Am J Gastroenterol* 2020; **115**: 322-339 [PMID: 32022720 DOI: 10.14309/ajg.0000000000000535]
8 **Comfort MW**, Gambill EE, Baggenstoss AH. Chronic relapsing pancreatitis; a study of 29 cases without associated disease of the biliary or gastrointestinal tract. *Gastroenterology* 1946; **6**: 376-408 [PMID: 20985712]
9 **Whitcomb DC**, Frulloni L, Garg P, Greer JB, Schneider A, Yadav D, Shimosegawa T. Chronic pancreatitis: An international draft consensus proposal for a new mechanistic definition. *Pancreatology* 2016; **16**: 218-224 [PMID: 26924663 DOI: 10.1016/j.pan.2016.02.001]
10 **Singh VK**, Yadav D, Garg PK. Diagnosis and Management of Chronic Pancreatitis: A Review. *JAMA* 2019; **322**: 2422-2434 [PMID: 31860051 DOI: 10.1001/jama.2019.19411]
11 **Khatkov IE**, Bordin DS, Lesko KA, Dubtsova EA, Karnaukhov NS, Kiriukova MA, Makarenko NV, Dorofeev AS, Savina IV, Salimgereeva

DA, Shurygina EI, Vinokurova LV. Contrast-Enhanced Computed Tomography and Laboratory Parameters as Non-Invasive Diagnostic Markers of Pancreatic Fibrosis. *Diagnostics (Basel)* 2023; **13** [PMID: 37510179 DOI: 10.3390/diagnostics13142435]

12 **Kleeff J**, Whitcomb DC, Shimosegawa T, Esposito I, Lerch MM, Gress T, Mayerle J, Drewes AM, Rebours V, Akisik F, Muñoz JED, Neoptolemos JP. Chronic pancreatitis. *Nat Rev Dis Primers* 2017; **3**: 17060 [PMID: 28880010 DOI: 10.1038/nrdp.2017.60]

13 **Apte M**, Pirola RC, Wilson JS. Pancreatic stellate cell: physiologic role, role in fibrosis and cancer. *Curr Opin Gastroenterol* 2015; **31**: 416-423 [PMID: 26125317 DOI: 10.1097/MOG.0000000000000196]

14 **Schneider A**, Löhr JM, Singer MV. The M-Annheim classification of chronic pancreatitis: introduction of a unifying classification system based on a review of previous classifications of the disease. *J Gastroenterol* 2007; **42**: 101-119 [PMID: 17351799 DOI: 10.1007/s00535-006-1945-4]

15 **Tuck NL**, Teo K, Kuhlmann L, Olesen SS, Johnson M, Bean DJ, Rashid U, MacCormick AD, Srikumar G, Drewes AM, Windsor JA. Pain patterns in chronic pancreatitis and chronic primary pain. *Pancreatology* 2022; **22**: 572-582 [PMID: 35562269 DOI: 10.1016/j.pan.2022.04.016]

16 **Mullady DK**, Yadav D, Amann ST, O'Connell MR, Barmada MM, Elta GH, Scheiman JM, Wamsteker EJ, Chey WD, Korneffel ML, Weinman BM, Slivka A, Sherman S, Hawes RH, Brand RE, Burton FR, Lewis MD, Gardner TB, Gelrud A, DiSario J, Baillie J, Banks PA, Whitcomb DC, Anderson MA; NAPS2 Consortium. Type of pain, pain-associated complications, quality of life, disability and resource utilisation in chronic pancreatitis: a prospective cohort study. *Gut* 2011; **60**: 77-84 [PMID: 21148579 DOI: 10.1136/gut.2010.213835]

17 **Wilcox CM**, Yadav D, Ye T, Gardner TB, Gelrud A, Sandhu BS, Lewis MD, Al-Kaade S, Cote GA, Forsmark CE, Guda NM, Conwell DL, Banks PA, Muniraj T, Romagnuolo J, Brand RE, Slivka A, Sherman S, Wisniewski SR, Whitcomb DC, Anderson MA. Chronic pancreatitis pain pattern and severity are independent of abdominal imaging findings. *Clin Gastroenterol Hepatol* 2015; **13**: 552-60; quiz e28 [PMID: 25424572 DOI: 10.1016/j.cgh.2014.10.015]

18 **Bahuva R**, Walsh RM, Kapural L, Stevens T. Morphologic abnormalities are poorly predictive of visceral pain in chronic pancreatitis. *Pancreas* 2013; **42**: 6-10 [PMID: 22750976 DOI: 10.1097/MPA.0b013e318258cd9c]

19 **Mann R**, Boregowda U, Vyas N, Gajendran M, Umapathy CP, Sayana H, Echavarria J, Patel S, Saligram S. Current advances in the management of chronic pancreatitis. *Dis Mon* 2021; **67**: 101225 [PMID: 34176572 DOI: 10.1016/j.disamonth.2021.101225]

20 **Anderson MA**, Akshintala V, Albers KM, Amann ST, Belfer I, Brand R, Chari S, Cote G, Davis BM, Frulloni L, Gelrud A, Guda N, Humar A, Liddle RA, Slivka A, Gupta RS, Szigethy E, Talluri J, Wassef W, Wilcox CM, Windsor J, Yadav D, Whitcomb DC. Mechanism, assessment and management of pain in chronic pancreatitis: Recommendations of a multidisciplinary study group. *Pancreatology* 2016; **16**: 83-94 [PMID: 26620965 DOI: 10.1016/j.pan.2015.10.015]

21 **Drewes AM**, van Veldhuisen CL, Bellin MD, Besselink MG, Bouwense SA, Olesen SS, van Santvoort H, Vase L, Windsor JA. Assessment of pain associated with chronic pancreatitis: An international consensus guideline. *Pancreatology* 2021; **21**: 1256-1284 [PMID: 34391675 DOI: 10.1016/j.pan.2021.07.004]

22 **Ammann RW**, Akovbiantz A, Largiader F, Schueler G. Course and outcome of chronic pancreatitis. Longitudinal study of a mixed medical-surgical series of 245 patients. *Gastroenterology* 1984; **86**: 820-828 [PMID: 6706066]

23 **Ammann RW**, Buehler H, Muench R, Freiburghaus AW, Siegenthaler W. Differences in the natural history of idiopathic (nonalcoholic) and alcoholic chronic pancreatitis. A comparative long-term study of 287 patients. *Pancreas* 1987; **2**: 368-377 [PMID: 3628234 DOI: 10.1097/00006676-198707000-00002]

24 **Lankisch PG**, Löhr-Happe A, Otto J, Creutzfeldt W. Natural course in chronic pancreatitis. Pain, exocrine and endocrine pancreatic insufficiency and prognosis of the disease. *Digestion* 1993; **54**: 148-155 [PMID: 8359556 DOI: 10.1159/000201029]

25 **Lankisch PG**, Seidensticker F, Löhr-Happe A, Otto J, Creutzfeldt W. The course of pain is the same in alcohol- and nonalcohol-induced chronic pancreatitis. *Pancreas* 1995; **10**: 338-341 [PMID: 7792289 DOI: 10.1097/00006676-199505000-00003]

26 **Dimcevski G**, Sami SA, Funch-Jensen P, Le Pera D, Valeriani M, Arendt-Nielsen L, Drewes AM. Pain in chronic pancreatitis: the role of reorganization in the central nervous system. *Gastroenterology* 2007; **132**: 1546-1556 [PMID: 17408654 DOI: 10.1053/j.gastro.2007.01.037]

27 **Sarner M**, Cotton PB. Classification of pancreatitis. *Gut* 1984; **25**: 756-759 [PMID: 6735257 DOI: 10.1136/gut.25.7.756]

28 **Olesen SS**, Steinkohl E, Hansen TM, Drewes AM, Frøkjær JB. Single- and multiparameter magnetic resonance imaging for diagnosing and severity grading of chronic pancreatitis. *Abdom Radiol (NY)* 2023; **48**: 630-641 [PMID: 36477631 DOI: 10.1007/s00261-022-03760-6]

29 **Whitcomb DC**, Shimosegawa T, Chari ST, Forsmark CE, Frulloni L, Garg P, Hegyi P, Hirooka Y, Irisawa A, Ishikawa T, Isaji S, Lerch MM, Levy P, Masamune A, Wilcox CM, Windsor J, Yadav D, Sheel A, Neoptolemos JP; Working Group for the International (IAP – APA – JPS – EPC) Consensus Guidelines for Chronic Pancreatitis. International consensus statements on early chronic Pancreatitis. Recommendations from the working group for the international consensus guidelines for chronic pancreatitis in collaboration with The International Association of Pancreatology, American Pancreatic Association, Japan Pancreas Society, PancreasFest Working Group and European Pancreatic Club. *Pancreatology* 2018; **18**: 516-527 [PMID: 29793839 DOI: 10.1016/j.pan.2018.05.008]

30 **Shimizu K**, Ito T, Irisawa A, Ohtsuka T, Ohara H, Kanno A, Kida M, Sakagami J, Sata N, Takeyama Y, Tahara J, Hirota M, Fujimori N, Masamune A, Mochida S, Enomoto N, Shimosegawa T, Koike K. Evidence-based clinical practice guidelines for chronic pancreatitis 2021. *J Gastroenterol* 2022; **57**: 709-724 [PMID: 35994093 DOI: 10.1007/s00535-022-01911-6]

31 **Liu C**, Shi Y, Lan G, Xu Y, Yang F. Evaluation of Pancreatic Fibrosis Grading by Multiparametric Quantitative Magnetic Resonance Imaging. *J Magn Reson Imaging* 2021; **54**: 1417-1429 [PMID: 33819364 DOI: 10.1002/jmri.27626]

32 **Tirkes T**, Lin C, Fogel EL, Sherman SS, Wang Q, Sandrasegaran K. T(1) mapping for diagnosis of mild chronic pancreatitis. *J Magn Reson Imaging* 2017; **45**: 1171-1176 [PMID: 27519287 DOI: 10.1002/jmri.25428]

33 **Wang N**, Gaddam S, Xie Y, Christodoulou AG, Wu C, Ma S, Fan Z, Wang L, Lo S, Hendifar AE, Pandol SJ, Li D. Multitasking dynamic contrast enhanced magnetic resonance imaging can accurately differentiate chronic pancreatitis from pancreatic ductal adenocarcinoma. *Front Oncol* 2022; **12**: 1007134 [PMID: 36686811 DOI: 10.3389/fonc.2022.1007134]

34 **Bornman PC**, Marks IN, Girdwood AH, Clain JE, Narunsky L, Clain DJ, Wright JP. Is pancreatic duct obstruction or stricture a major cause of pain in calcific pancreatitis? *Br J Surg* 1980; **67**: 425-428 [PMID: 7388340 DOI: 10.1002/bjs.1800670614]

35 **Jensen AR**, Matzen P, Malchow-Møller A, Christoffersen I. Pattern of pain, duct morphology, and pancreatic function in chronic pancreatitis. A comparative study. *Scand J Gastroenterol* 1984; **19**: 334-338 [PMID: 6740208]

36 **Morgan DE**, Smith JK, Hawkins K, Wilcox CM. Endoscopic stent therapy in advanced chronic pancreatitis: relationships between ductal changes, clinical response, and stent patency. *Am J Gastroenterol* 2003; **98**: 821-826 [PMID: 12738462 DOI: 10.1111/j.1572-0241.2003.07381.x]

37 **Malfertheiner P**, Büchler M, Stanescu A, Ditschuneit H. Pancreatic morphology and function in relationship to pain in chronic pancreatitis. *Int*

J Pancreatol 1987; **2**: 59-66 [PMID: 3681034 DOI: 10.1007/BF02788349]

38 **Demir IE**, Friess H, Ceyhan GO. Neural plasticity in pancreatitis and pancreatic cancer. *Nat Rev Gastroenterol Hepatol* 2015; **12**: 649-659 [PMID: 26460352 DOI: 10.1038/nrgastro.2015.166]

39 **Frøkjær JB**, Olesen SS, Drewes AM. Fibrosis, atrophy, and ductal pathology in chronic pancreatitis are associated with pancreatic function but independent of symptoms. *Pancreas* 2013; **42**: 1182-1187 [PMID: 24048457 DOI: 10.1097/MPA.0b013e31829628f4]

World Journal of Radiology

Submit a Manuscript: https://www.f6publishing.com

World J Radiol 2024 March 28; 16(3): 49-57

DOI: 10.4329/wjr.v16.i3.49

ISSN 1949-8470 (online)

ORIGINAL ARTICLE

Retrospective Study

Evaluating pediatric ureteropelvic junction obstruction: Dynamic magnetic resonance urography *vs* renal scintigraphy 99m-technetium mercaptoacetyltriglycine

Yousuf Al-Shaqsi, Matthieu Peycelon, Annabel Paye-Jaouen, Elisabeth Carricaburu, Anca Tanase, Christine Grapin-Dagorno, Alaa El-Ghoneimi

Specialty type: Radiology, nuclear medicine and medical imaging

Provenance and peer review: Unsolicited article; Externally peer reviewed.

Peer-review model: Single blind

Peer-review report's scientific quality classification

Grade A (Excellent): 0
Grade B (Very good): 0
Grade C (Good): C
Grade D (Fair): D
Grade E (Poor): 0

P-Reviewer: Aydin S, Turkey; Nazir Z, Pakistan

Received: November 20, 2023
Peer-review started: November 20, 2023
First decision: December 19, 2023
Revised: January 18, 2024
Accepted: March 12, 2024
Article in press: March 12, 2024
Published online: March 28, 2024

Yousuf Al-Shaqsi, Department of Pediatric Surgery, Sultan Qaboos University Hospital, Muscat 123, Oman

Yousuf Al-Shaqsi, Matthieu Peycelon, Annabel Paye-Jaouen, Elisabeth Carricaburu, Christine Grapin-Dagorno, Alaa El-Ghoneimi, Service de Chirurgie Viscérale et Urologie Pédiatrique, Hôpital Universitaire Robert-Debré, Assistance-Publique Hôpitaux de Paris, Paris 75019, France

Yousuf Al-Shaqsi, Matthieu Peycelon, Annabel Paye-Jaouen, Anca Tanase, Alaa El-Ghoneimi, Centre de Références Maladies Rares, Malformations Rares des Voies Urinaires (MARVU), Paris 97019, France

Matthieu Peycelon, Alaa El-Ghoneimi, Faculté de Médecine, Université de Paris, Paris 75006, France

Anca Tanase, Service d'Imagerie Pédiatrique, Hôpital Universitaire Robert-Debré, Assistance-Publique Hôpitaux de Paris, Paris 75019, France

Christine Grapin-Dagorno, Université Paris 13, Sorbonne Paris Cité, Paris 75013, France

Corresponding author: Yousuf Al-Shaqsi, MD, Doctor, Surgeon, Department of Pediatric Surgery, Sultan Qaboos University Hospital, Alkhoud BO BOX 38, Muscat 123, Oman. y.alshaqsi@hotmail.com

Abstract

BACKGROUND

Ureteropelvic junction obstruction (UPJO) is a common congenital urinary tract disorder in children. It can be diagnosed as early as *in utero* due to the presence of hydronephrosis or later in life due to symptomatic occurrence.

AIM

To evaluate the discrepancy between dynamic contrast-enhanced magnetic resonance urography (dMRU) and scintigraphy 99m-technetium mercaptoacetyl-triglycine (MAG-3) for the functional evaluation of UPJO.

METHODS
Between 2016 and 2020, 126 patients with UPJO underwent surgery at Robert Debré Hospital. Of these, 83 received a prenatal diagnosis, and 43 were diagnosed during childhood. Four of the 126 patients underwent surgery based on the clinical situation and postnatal ultrasound findings without undergoing functional imaging evaluation. Split renal function was evaluated preoperatively using scintigraphy MAG-3 (n = 28), dMRU (n = 53), or both (n = 40). In this study, we included patients who underwent surgery for UPJO and scintigraphy MAG-3 + dMRU but excluded those who underwent only scintigraphy MAG-3 or dMRU. The patients were divided into groups A (< 10% discrepancy) and B (> 10% discrepancy). We examined the discrepancy in split renal function between the two modalities and investigated the possible risk factors.

RESULTS
The split renal function between the two kidneys was compared in 40 patients (28 boys and 12 girls) using scintigraphy MAG-3 and dMRU. Differential renal function, as determined using both modalities, showed a difference of < 10% in 31 children and > 10% in 9 children. Calculation of the relative renal function using dMRU revealed an excellent correlation coefficient with renal scintigraphy MAG-3 for both kidneys.

CONCLUSION
Our findings demonstrated that dMRU is equivalent to scintigraphy MAG-3 for evaluating split renal function in patients with UPJO.

Key Words: Uteropelvic junction obstruction; Scintigraphy 99m-technetium mercaptoacetyltriglycine; Magnetic resonance imaging; Dynamic contrast-enhanced magnetic resonance urography

©The Author(s) 2024. Published by Baishideng Publishing Group Inc. All rights reserved.

Core Tip: This study aimed to evaluate the discrepancy between dynamic contrast-enhanced magnetic resonance urography (MRU) and scintigraphy 99m-technetium mercaptoacetyltriglycine (MAG-3) in the functional evaluation of ureteropelvic junction obstruction (UPJO). The results show that dynamic contrast-enhanced MRU is equivalent to scintigraphy MAG-3 for evaluating split renal function in cases of UPJO in all pediatric age groups. Moreover, it is safe and accurate and does not require ionizing radiation.

Citation: Al-Shaqsi Y, Peycelon M, Paye-Jaouen A, Carricaburu E, Tanase A, Grapin-Dagorno C, El-Ghoneimi A. Evaluating pediatric ureteropelvic junction obstruction: Dynamic magnetic resonance urography *vs* renal scintigraphy 99m-technetium mercaptoacetyltriglycine. *World J Radiol* 2024; 16(3): 49-57
URL: https://www.wjgnet.com/1949-8470/full/v16/i3/49.htm
DOI: https://dx.doi.org/10.4329/wjr.v16.i3.49

INTRODUCTION

Ureteropelvic junction obstruction (UPJO), the most common urinary tract disorder among children, is observed in all pediatric age groups[1,2]. It can be diagnosed during the neonatal period due to the presence of prenatal dilation of the upper urinary tract or later in life due to symptomatic occurrence. However, most cases are detected during the perinatal period[1,3].

Renal ultrasound is generally used to detect and follow up hydronephrosis, whereas renal scintigraphy using dimercaptosuccinic acid or 99m-technetium mercaptoacetyltriglycine (MAG-3) evaluates renal function and obstruction, respectively[4,5]. Computed tomography can be an option for adolescents and young adults to assess obstruction and identify any aberrant vessels as a cause of UPJO or for postoperative follow-up[4]. Although these techniques can clearly assess obstructions, they cannot predict the progressive loss of renal function or determine which patients will benefit from surgery.

The decision for surgical intervention to correct UPJO is controversial; while some surgeons suggest early intervention, others promote a wait-and-see approach[5,6]. Many urologists follow the sonographic diagnosis of hydronephrotic kidney and use declining renal function in functional imaging studies as an indication for surgery[6]. Asymptomatic patients with UPJO should only be treated if there is evidence of asymmetric function, functional deterioration, or hydronephrosis[4-7]. Identifying and surgically correcting UPJO in these patients before the occurrence of nephron loss is essential.

Renal scintigraphy is considered the gold standard technique for evaluating anatomical obstruction and measuring split renal function in children and adults, driving therapeutic decisions[8-10]. However, dynamic contrast-enhanced magnetic resonance urography (dMRU) has recently been proposed as an alternative technique for evaluating the drainage curve and split renal function in obstructive uropathy, without requiring ionizing radiation[11-13]. The use of

dMRU to obtain both anatomical and functional information in a single examination without radiation is beneficial, especially in the follow-up of young patients[14,15].

This study aimed to evaluate the discrepancies between dMRU and renal scintigraphy MAG-3 for the functional evaluation of UPJO in children. We hypothesized that dMRU and renal scintigraphy MAG-3 would provide similar information regarding renal function.

MATERIALS AND METHODS

This retrospective cohort study included patients with UPJO who underwent surgery and renal scintigraphy MAG-3 + dMRU at Roberts Debré Children University Hospital between January 2016 and March 2020 but excluded those who underwent only renal scintigraphy MAG-3 or dMRU (Figure 1). This retrospective study was conducted in accordance with the ethical principles outlined in the Helsinki Declaration. Due to the nature of the study involving analysis of de-identified data from existing medical records, formal ethical approval from an institutional review board was not sought. However, efforts were made to ensure patient confidentiality and respect for individual privacy throughout the study process.

First, all patients underwent renal ultrasonography for the initial radiological evaluation of renal pelvic dilatation (Table 1). Those suspected of UPJO were then subjected to further renal function evaluations using scintigraphy MAG-3 or dMRU based on the available modality and the radiologist's experience. As these patients did not require surgical correction of the UPJO, they were followed up in the clinic with renal ultrasonography. However, in situations where the patients had major dilatation of the renal pelvis on ultrasound findings during follow-up, we requested another modality for comparison *i.e.*, if the patient had initially underwent scintigraphy MAG-3, we requested dMRU, and vice versa (Table 2).

We then examined the discrepancies in split renal function assessments between the two radiological modalities. To assess split renal function in both kidneys, functional dMRU results were correlated with the reference standard of MAG-3 scintigraphy. The patients were divided into two groups: Group A, the discrepancy between renal scintigraphy MAG-3 and dMRU was < 10% (n = 31), and Group B, the discrepancy was > 10% (n = 9). In addition, we investigated the potential risk factors for these discrepancies, including sex, age at diagnosis, preoperative febrile urinary tract infection, presence of vesicoureteral reflux, and associated anomalies of the urinary tract, such as duplication of the urinary system, single kidney, and horseshoe kidney (Table 3).

dMRU protocol

dMRU is performed as an outpatient study or in the day care unit, depending on the child's age and the need for sedation. Children < 7 years of age required sedation and observation during daycare for a few hours before discharge from the hospital. Chloral hydrate 50–75 mg/kg PO was administered to children < 1 year of age 30–60 min before the procedure and repeated for 30 min if necessary. In older children, we administered intrarectal pentobarbital (5 mg/kg) and alimemazine (2 mg/kg) 1–2 h before the procedure.

Sedation was induced and monitored by a trained pediatric sedation nurse. The patients were continuously monitored for oxygen saturation and pulse rate. All children were hydrated before the study with Ringer's lactate solution (10 mL/kg) and premedicated with phenobarbitone (5 mg/kg) administered intrarectally 30 min before the procedure. First, T2-weighted imaging sequences [static magnetic resonance urography (MRU)] were performed to evaluate the entire urinary tract system. Next, furosemide (1 mg/kg) was administered intravenously 1 min after the injection of gadolinium-DTPA 0.05 mmol/kg. Then, routine T1 imaging (excretory MRU) of the kidneys, ureters, and bladder was performed 10 min after furosemide injection. Sequential dynamic contrast-enhanced imaging with a time resolution of 15 s was performed using the volumetric gradient echo technique covering the entire urinary tract. This volumetric sequence was repeated continuously for the initial 3 min following a bolus injection of gadolinium-DTPA 0.05 mmol/kg. Datasets were then obtained at 1 min intervals for a total of 20 min. Renal and ureteral transition times were measured, and the split renal function between the two kidneys was calculated using ImageJ software.

Scintigraphy MAG-3 protocol

A urinary catheter was placed, and the children were orally hydrated with 10–20 mL/kg of water 30–40 min before the study. Posterior dynamic acquisition was performed after intravenous injection of MAG-3 3.7 MBq/kg and furosemide (1 mg/kg). The patients were placed in the supine position with their backs facing the camera. Serial 15–30 s images were acquired for 30–60 min, depending on the technique chosen. In the dynamic renal study, careful evaluation of the parenchymal phase using the Patlak–Rutland method revealed split renal function. Cortical transit time and collection system dilatation were examined during the excretory phase (initial 2–4 min). Baseline images of the diuretic phase were used to assess the diuretic effects.

Statistical analysis

Descriptive statistics were performed using Fisher's exact test or the χ^2 tests for categorical variables, Student's t-test for parametric continuous data (presented as mean and standard deviation), and the Mann–Whitney test for nonparametric continuous data [presented as median and interquartile range (IQR)]. A positive correlation coefficient was observed at r > 0. Potential risk factors for discrepancies in renal function between renal scintigraphy MAG-3 and dMRU were analyzed using univariate analysis, with P < 0.05 considered statistically significant. On exploratory analysis, all variables with values of P < 0.20 on univariate analysis were assessed for a possible association with the discrepancy in renal

Table 1 Characteristics of the entire study cohort, *n* (%)

	Entire cohort, *n* = 126	Scintigraphy MAG-3 only, *n* = 28	DMRU only, *n* = 54	Scintigraphy MAG-3 + dMRU, *n* = 40	*P* value[a]
Sex					0.837
M	88 (70)	18 (64)	38(70)	28 (70)	
F	38 (30)	10 (36)	16 (30)	12 (30)	
Age at diagnosis, months	22 (8-112)	8 (4-70)	29 (8-119)	30 (14-127)	0.0471
Diagnosis					
Prenatal	83 (66)	18 (64)	30 (55.5)	31 (77)	0.146
Postnatal	43 (34)	10 (36)	24 (44.5)	9 (21.5)	
Associated anomalies					0.0476
Duplication of urinary system	3 (2.4)	0	3 (5.5)	0	
Ureterocele	0	0	0	0	
Single kidney	2 (1.6)	0	1 (2)	1 (2.5)	
Horseshoe kidney	1 (0.8)	0	1 (2)	0	
Vesicoureteral reflux	3 (2.4)	0	0	3 (7.5)	
Pyelonephritis	21 (17)	2 (7)	12 (22)	7 (17.5)	0.241
Urinary stones	3 (2.4)	1 (4)	1 (2)	1 (2.5)	0.999
Follow-up, months	11 (3-23)	8 (3-27)	11 (4-19)	12 (5-20)	0.966

[a]*P* value: Common presentation of ureteropelvic junction obstruction in the entire study cohort ($P < 0.05$ was considered statistically significant).
Values are presented as median (interquartile range) or *n* (%), as appropriate. dMRU: Dynamic contrast-enhanced magnetic resonance urography; F: Female; M: Male; MAG-3: 99m-technetium mercaptoacetyltriglycine.

Table 2 Decision-making for surgical correction of ureteropelvic junction obstruction, *n* (%)

	MAG-3 primary, *n* = 30 (75)	DMRU secondary, *n* = 30 (75)	DMRU primary, *n* = 10 (25)	MAG-3 secondary, *n* = 10 (25)
Affected kidney	42 (28-48)	42 (22-50)	22 (15-40)	38 (31-45)
Age, months	13 (4-48)	29 (9-109)	41 (11-129)	12 (4-116)
Affected renal size, mm				
RUS	28 (24-35)	XY	28.5 (13)	XY
MRI		28 (21-35)		
Before furosemide		30 (24-38)		26 (11)
After furosemide				30 (17)
Surgical decision	No	Yes	No	Yes

Values are shown as median (interquartile range). DMRU: Dynamic contrast-enhanced magnetic resonance urography; MAG-3: 99m-technetium mercaptoacetyltriglycine; MRI: Magnetic resonance imaging; RUS: Renal ultrasonography.

function between renal scintigraphy MAG-3 and dMRU on multivariate Cox regression.

RESULTS

A total of 126 patients were included in the study. Of these patients, 83 were diagnosed prenatally, and 43 (34%) were diagnosed later during childhood (median age, 9 years). Four (3%) of 126 patients underwent surgery based on clinical evaluation and postnatal ultrasound findings, without undergoing any functional imaging evaluation. Split renal

Table 3 Characteristics of the patients enrolled in the study (*n* = 40), *n* (%)

	Scintigraphy MAG-3 + dMRU, *n* = 40	Group A < 10% discrepancy, *n* = 31	Group B > 10% discrepancy, *n* = 9	*P* value[a]
Sex				0.697
M	28 (70)	21 (75)	7 (25)	
F	12 (30)	10 (83)	2 (17)	
Age at surgery, months	30 (14-127)	37 (14-134)	27 (13-76)	0.641
Diagnosis				0.0897
Prenatal	31 (77.5)	22 (71)	9 (29)	
Postnatal	9 (22.5)	9 (29)	0	
Associated anomalies				0.999
Duplication of urinary system	0	0	0	
Ureterocele	0	0	0	
Single kidney	1 (2.5)	1 (3)	0	
Horseshoe kidney	0	0	0	
Vesicoureteral reflux	3 (7.5)	1 (3)	2 (22)	0.999
Pyelonephritis	7 (17.5)	6 (19)	1 (11)	0.999
Urinary stones	1 (2.5)	1 (3)	0	0.999
Follow-up, months	12 (5-20)	10 (3-16)	19 (10-26)	0.05

[a]*P* value: Potential risk factors for a discrepancy in renal function between group A and group B ($P < 0.05$ was considered statistically significant). Values are shown as *n* (%) or median (interquartile range), as appropriate. Group A: Discrepancy in renal function between scintigraphy and dynamic contrast-enhanced magnetic resonance urography (dMRU) is < 10%. Group B: Discrepancy in renal function between scintigraphy and dMRU is > 10%. dMRU: Dynamic contrast-enhanced magnetic resonance urography; MAG-3: 99m-technetium mercaptoacetyltriglycine; F: Female; M: Male.

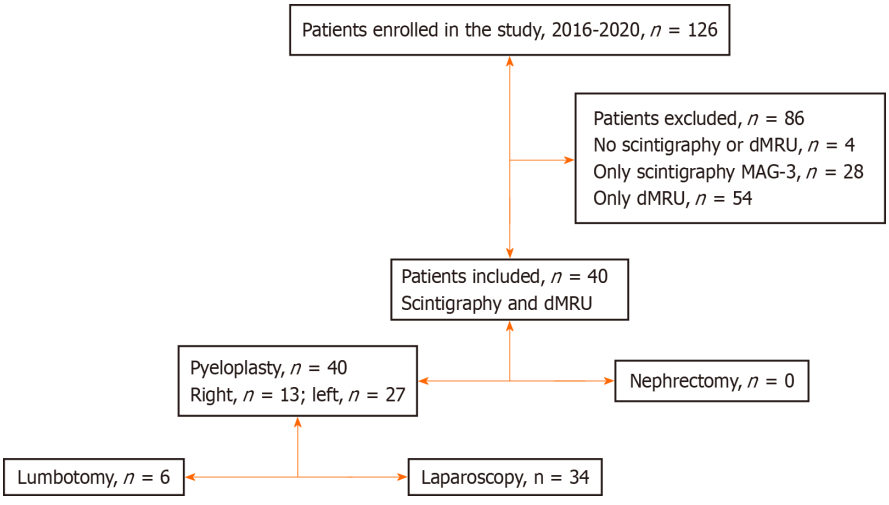

Figure 1 Overview of the study enrollment process. dMRU: Dynamic contrast-enhanced magnetic resonance urography; MAG-3: 99m-technetium mercaptoacetyltriglycine.

function was evaluated preoperatively using an isotope renal scan [*n* = 28 (22%)], dynamic MRI [*n* = 54 (43%)], or both [*n* = 40 (32%)]. The most common presentation of UPJO was prenatal hydronephrosis in 83 (66%) patients, followed by lumbar pain in 22 (17%) and urinary tract infections in 21 (16%) ($P > 0.05$). Of the 126 patients, 4 (3%) had duplex systems, 1 had UPJO in a horseshoe kidney, 3 (2%) had vesicoureteral reflux, and 3 (3%) had urinary calculi ($P < 0.05$; Table 1).

Split renal function was compared in 40 patients [28 boys and 12 girls ($P > 0.05$)] using scintigraphy MAG-3 and dMRU. Of these, 31 (77%) received a prenatal diagnosis, and 9 (23%) were diagnosed during later childhood ($P > 0.05$). Differential renal function, as determined by scintigraphy MAG-3 and dMRU, differed by < 10% in 31 children and > 10%

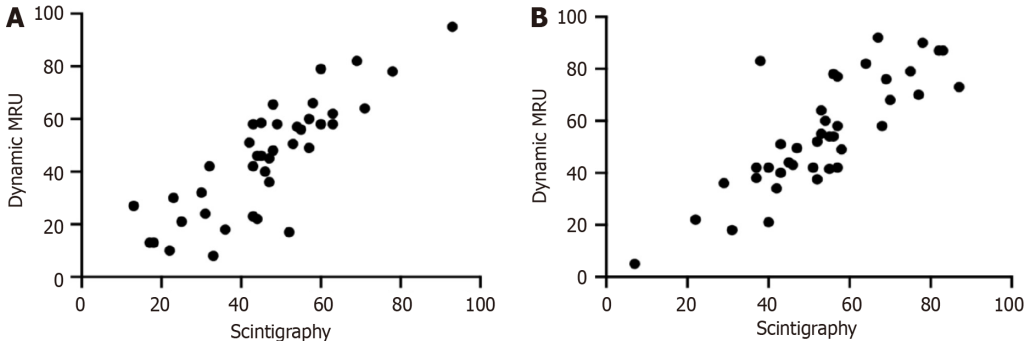

Figure 2 Relative differential function results on dynamic contrast-enhanced magnetic resonance urography *vs* scintigraphy. A: Relative differential function results of left kidney on dynamic contrast-enhanced magnetic resonance urography (dMRU) *vs* scintigraphy (correlation coefficient = 0.84); B: Relative differential function results of right kidney on dMRU *vs* scintigraphy (correlation coefficient = 0.82). MRU: Magnetic resonance urography.

in 9 children ($P > 0.05$; Table 3).

All patients underwent pyeloplasty [right side ($n = 13$) and left side ($n = 27$); $P > 0.05$] at a median age of 30 months (IQR, 14–127 months). Thirty-four patients underwent laparoscopy (retroperitoneoscopy or robot-assisted retroperitoneoscopy) while the other six underwent lumbotomy. Most patients (95%) had good clinical outcomes and satisfactory results on ultrasonography during follow-up [median, 12 months (IQR, 5–20 months)], and there were two cases (5%) of persistent renal pelvic dilatation without renal function degradation. Calculation of relative renal function by dMRU revealed an excellent correlation coefficient with renal scintigraphy MAG-3 for both kidneys ($r = 0.84$ and $r = 0.82$, respectively; Figure 2).

DISCUSSION

Congenital uropathy is a wide-spectrum entity that varies from asymptomatic to self-resolving and life-threatening conditions. Hydronephrosis is the most common congenital anomaly detected using ultrasonography during the prenatal period. While most cases of grade 1 and grade 2 hydronephrosis (96%) spontaneously resolve in the first year of life, a minority of patients develop UPJO[16]. Dynamic renal scintigraphy MAG-3 is considered the gold standard for estimating differential renal function and diagnosing obstructions in children. However, in recent times, dMRU has emerged as an alternative technique for evaluating the drainage curve and split renal function in obstructive uropathy[11-13]. dMRU provides excellent anatomical information on the urinary tract and enables the precise exclusion of urinary tract obstruction, without requiring ionizing radiation[16]. It produces high-resolution images arising from the accumulation of bright contrast content in the collection system and ureter, which enables identification of the ureter distal to the obstruction site[15]. Since 2000, dMRU has been the main modality for evaluating renal function at the Robertson Debré Children University Hospital. However, despite its benefits, dMRU is not widely used because it is expensive and there is a lack of trained pediatric radiologists.

Few studies have investigated the diagnostic value of dMRU for obstructive uropathy. For instance, Perez-Brayfield *et al*[13] reported that dMRU provides superior anatomical details compared with sonography and nuclear scintigraphy. Although the procedure requires sedation in all cases, it delivers no ionizing radiation to the infant or child. In this study, we examined the discrepancy in functional evaluation between dynamic contrast-enhanced MRU and renal scintigraphy MAG-3 in patients with UPJO who underwent surgery at our hospital over the last 4 years. From a total of 126 patients in the study, only 40 were included in the final analysis. We found a positive correlation coefficient in the relative differential of split renal function between the two modalities. Similarly, El-Nahas *et al*[12] reported that dMRU analysis of renal function had comparable results to those obtained with renal scintigraphy but superior spatial and contrast resolution. dMRU may be more sensitive than renal scintigraphy for analyzing poorly functional renal collecting systems. In addition to the earlier advantages of dMRU, we found that it is equivalent to nuclear medicine in evaluating split renal function and obstruction (Table 4). Thus, dMRU is a feasible radiological modality for the functional and anatomical evaluation of UPJO. Moreover, it is safe, accurate, and does not require exposure to ionizing radiation. However, the procedure requires sedation and short-term hospitalization. The limitations of this study include a small sample size from a single institution. The requirement for sedation during dMRU presents a practical challenge. Future implications emphasize the need for larger multicenter studies to confirm these findings, while advancements in imaging technology hold promise for enhancing the accessibility and viability of dMRU as a gold standard diagnostic tool for UPJO.

CONCLUSION

dMRU is equivalent to scintigraphy MAG-3 for evaluating split renal function in UPJO cases of all pediatric age groups. We found that the discrepancies and similarities in renal function were not significantly related to age at diagnosis, sex, or pyelonephritis. We believe that dMRU is an excellent alternative modality for the anatomical and functional evaluation of

Table 4 Discrepant characteristics of group A and group B, *n* (%)

	Scintigraphy MAG-3 + dMRU, *n* = 40	Group A < 10% discrepancy, *n* = 31	Group B > 10% discrepancy, *n* = 9	*P* value
Number of discrepancies	6.5 (2-9.8)	4 (2-8)	18 (12-24)	< 0.0001
Side				0.999
Right	13 (33)	10 (32)	3 (33)	
Left	27 (67)	21 (68)	6 (67)	
Renal transit (affected), s	100 (67-120)	100 (60-120)	100 (70-180)	0.359
Ureteral transit (affected), s	240 (180-511)	240 (180-520)	406 (300-511)	0.285
Affected renal size, mm				
RUS	28 (23-36)	29 (24-36)	24 (22-32)	0.381
MRI				
Before furosemide	28 (22-35)	31 (21-35)	25 (23-31)	0.652
After furosemide	30 (24-40)	29 (24-42)	32.5 (25-36)	0.966
Follow-up, months	12 (5-20)	10 (3-16)	19 (10-26)	0.05

Values are presented as median (interquartile range) or *n* (%), as appropriate. dMRU: Dynamic contrast-enhanced magnetic resonance urography; MAG-3: 99m-technetium mercaptoacetyltriglycine; MRI: Magnetic resonance imaging; RUS: Renal ultrasonography.

children with UPJO. However, larger multicenter studies are required to strengthen and consolidate our findings.

ARTICLE HIGHLIGHTS

Research background

Ureteropelvic obstruction is a common pediatric condition, which can be due to congenital internal obstruction or external obstruction secondary to crossing vessels. This study aims to encourage the use of dynamic contrast-enhanced magnetic resonance urography (dMRU) as a modality, measuring renal function as effectively as 99m-technetium mercaptoacetyltriglycine (MAG-3) and providing a good anatomical study in cases of obstruction due to crossing vessels.

Research motivation

dMRU proves advantageous as an alternative modality for ureteropelvic junction obstruction (UPJO). However, enhanced accessibility and cost-effectiveness can be achieved through advancements in magnetic resonance imaging technology.

Research objectives

The optimal imaging modalities for preoperative functional and anatomical assessment of UPJO in pediatric patients.

Research methods

Analysis of data in patients who underwent surgery for UPJO and had both dMRU and scintigraphy MAG-3 for split renal function assessment.

Research results

dMRU is equivalent to scintigraphy MAG-3 for evaluating split renal function in UPJO cases of all pediatric age groups. Future implications emphasize the need for larger multicenter studies to confirm findings, while advancements in imaging technology hold promise for enhancing the accessibility and viability of dMRU as a gold standard diagnostic tool of UPJO.

Research conclusions

dMRU is an excellent alternative modality for the anatomical and functional evaluation of children with UPJO. A large sample size is required to confirm this hypothesis.

Research perspectives

To enhance the accessibility and viability of dMRU.

FOOTNOTES

Author contributions: Al-Shaqsi Y contributed to writing and editing; Peycelon M contributed to design and editing; Paye-Jaouen A, Carricaburu E, Tanase A, and Grapin-Dagorno C contributed to data collection and analyzing data; El-Ghoneimi A contributed to design and editing.

Institutional review board statement: This retrospective study was conducted in accordance with the ethical principles outlined in the Helsinki Declaration. Due to the nature of the study involving analysis of de-identified data from existing medical records, formal ethical approval from an institutional review board was not sought. However, efforts were made to ensure patient confidentiality and respect for individual privacy throughout the study process.

Informed consent statement: Informed consent was waived for this retrospective study as it involved the analysis of de-identified data obtained from existing medical records. The study was conducted in accordance with ethical principles and guidelines outlined in the Helsinki Declaration.

Conflict-of-interest statement: All the authors report no relevant conflicts of interest for this article.

Data sharing statement: No additional data are available.

Open-Access: This article is an open-access article that was selected by an in-house editor and fully peer-reviewed by external reviewers. It is distributed in accordance with the Creative Commons Attribution NonCommercial (CC BY-NC 4.0) license, which permits others to distribute, remix, adapt, build upon this work non-commercially, and license their derivative works on different terms, provided the original work is properly cited and the use is non-commercial. See: https://creativecommons.org/Licenses/by-nc/4.0/

Country/Territory of origin: France

ORCID number: Yousuf Al-Shaqsi 0000-0003-1846-3129.

S-Editor: Li L
L-Editor: Webster JR
P-Editor: Zhao S

REFERENCES

1 **Groth TW**, Mitchell ME. Ureteropelvic junction obstruction. In: Coran A, editor. Paediatric Surgery. 7th ed. Philadelphia: Elsevier, 2012: 1411-1425 [DOI: 10.1016/B978-0-323-07255-7.00113-6]
2 **Zderic SA**, Lambert SM. Developmental abnormalities of the genitourinary system. In: Gleason CA, Devaskar SU, editor. Avery's Diseases of the Newborn. 9th ed. Philadelphia: Elsevier, 2012: 1191-1204 [DOI: 10.1016/B978-1-4377-0134-0.10084-8]
3 **Brown T**, Mandell J, Lebowitz RL. Neonatal hydronephrosis in the era of sonography. *AJR Am J Roentgenol* 1987; **148**: 959-963 [PMID: 3034009 DOI: 10.2214/ajr.148.5.959]
4 **Lawler LP**, Jarret TW, Corl FM, Fishman EK. Adult ureteropelvic junction obstruction: insights with three-dimensional multi-detector row CT. *Radiographics* 2005; **25**: 121-134 [PMID: 15653591 DOI: 10.1148/rg.251045510]
5 **González R**, Schimke CM. Ureteropelvic junction obstruction in infants and children. *Pediatr Clin North Am* 2001; **48**: 1505-1518 [PMID: 11732127 DOI: 10.1016/S0031-3955(05)70388-6]
6 **Gopal M**, Peycelon M, Caldamone A, Chrzan R, El-Ghoneimi A, Olsen H, Leclair MD, Stillebroer A, MacDonald C, Tonnhofer U, Strasser C, Adam A, Spinoit AF, Haid B. Management of ureteropelvic junction obstruction in children-a roundtable discussion. *J Pediatr Urol* 2019; **15**: 322-329 [PMID: 31227314 DOI: 10.1016/j.jpurol.2019.05.010]
7 **Metcalfe PD**, Assmus M, Kiddoo D. Symptomatic *vs* asymptomatic pyeloplasties: A single institution review. *Can Urol Assoc J* 2014; **8**: 428-431 [PMID: 25553157 DOI: 10.5489/cuaj.2271]
8 **Atılgan HI**, Koca G, Demirel K, Ozyurt S, Yildirim Ş, Orak R, Baskın A, Korkmaz M. Comparative evaluation of differential renal functions and renal parenchymal defects by using the Tc-99m DMSA and Tc-99m MAG3 scintigraphies. *Kafkas J Med Sci* 2012; **2**: 43-48 [DOI: 10.5505/kjms.2012.21939]
9 **O'Reilly PH**, Lawson RS, Shields RA, Testa HJ. Idiopathic hydronephrosis--the diuresis renogram: a new non-invasive method of assessing equivocal pelvioureteral junction obstruction. *J Urol* 1979; **121**: 153-155 [PMID: 423326 DOI: 10.1016/S0022-5347(17)56703-8]
10 **Sharfuddin A**. Renal relevant radiology: imaging in kidney transplantation. *Clin J Am Soc Nephrol* 2014; **9**: 416-429 [PMID: 24202132 DOI: 10.2215/CJN.02960313]
11 **Rohrschneider WK**, Hoffend J, Becker K, Clorius JH, Darge K, Kooijman H, Tröger J. Combined static-dynamic MR urography for the simultaneous evaluation of morphology and function in urinary tract obstruction. I. Evaluation of the normal status in an animal model. *Pediatr Radiol* 2000; **30**: 511-522 [PMID: 10993535 DOI: 10.1007/s002470000270]
12 **El-Nahas AR**, Abou El-Ghar ME, Refae HF, Gad HM, El-Diasty TA. Magnetic resonance imaging in the evaluation of pelvi-ureteric junction obstruction: an all-in-one approach. *BJU Int* 2007; **99**: 641-645 [PMID: 17407519 DOI: 10.1111/j.1464-410X.2006.06673.x]
13 **Perez-Brayfield MR**, Kirsch AJ, Jones RA, Grattan-Smith JD. A prospective study comparing ultrasound, nuclear scintigraphy and dynamic contrast enhanced magnetic resonance imaging in the evaluation of hydronephrosis. *J Urol* 2003; **170**: 1330-1334 [PMID: 14501762 DOI: 10.1097/01.ju.0000086775.66329.00]
14 **El-Diasty T**, Mansour O, Farouk A. Diuretic contrast-enhanced magnetic resonance urography *vs* intravenous urography for depiction of nondilated urinary tracts. *Abdom Imaging* 2003; **28**: 135-145 [PMID: 12483401 DOI: 10.1007/s00261-002-0010-x]

15 **Sidhu G**, Beyene J, Rosenblum ND. Outcome of isolated antenatal hydronephrosis: a systematic review and meta-analysis. *Pediatr Nephrol* 2006; **21**: 218-224 [PMID: 16362721 DOI: 10.1007/s00467-005-2100-9]

16 **Rodigas J**, Kirsch H, John U, Seifert P, Winkens T, Stenzel M, Mentzel HJ. Static and Functional MR Urography to Assess Congenital Anomalies of the Kidney and Urinary Tract in Infants and Children: Comparison With MAG3 Renal Scintigraphy and Sonography. *AJR Am J Roentgenol* 2018; **211**: 193-203 [PMID: 29702016 DOI: 10.2214/AJR.17.17891]

World Journal of Radiology

Submit a Manuscript: https://www.f6publishing.com

World J Radiol 2024 March 28; 16(3): 58-68

DOI: 10.4329/wjr.v16.i3.58

ISSN 1949-8470 (online)

CASE REPORT

Ductal carcinoma in situ within a fibroadenoma: A case report and review of literature

Yazmin Olivares-Antúnez, Yesika Janett Dávila-Zablah, José Raúl Vázquez-Ávila, Gabriela Sofía Gómez-Macías, María Teresa Mireles-Aguilar, Margarita Lilia Garza-Montemayor

Specialty type: Radiology, nuclear medicine and medical imaging

Provenance and peer review: Unsolicited article; Externally peer reviewed.

Peer-review model: Single blind

Peer-review report's scientific quality classification

Grade A (Excellent): 0
Grade B (Very good): B
Grade C (Good): C
Grade D (Fair): D
Grade E (Poor): 0

P-Reviewer: Tangsuwanaruk T, Thailand; Yap RV, Philippines

Received: December 10, 2023
Peer-review started: December 10, 2023
First decision: January 6, 2024
Revised: January 20, 2024
Accepted: March 6, 2024
Article in press: March 6, 2024
Published online: March 28, 2024

Yazmin Olivares-Antúnez, Yesika Janett Dávila-Zablah, Margarita Lilia Garza-Montemayor, Department of Diagnostic Breast Imaging Center, Hospital Zambrano Hellion, Tecnológico de Monterrey, Nuevo León 66260, Mexico

José Raúl Vázquez-Ávila, Gabriela Sofía Gómez-Macías, Department of Patology Service, Hospital San José, Tecnológico de Monterrey, Nuevo León 64710, Mexico

Gabriela Sofía Gómez-Macías, Department of Faculty of Medicine, Hospital Universitario de la UANL, Nuevo León 64710, Mexico.

María Teresa Mireles-Aguilar, Department of Breast Surgery Center, Hospital Zambrano Hellion, Tecnológico de Monterrey, Nuevo León 66260, Mexico

Corresponding author: Yazmin Olivares-Antúnez, MD, Staff Physician, Department of Diagnostic Breast Imaging Center, Hospital Zambrano Hellion, Tecnológico de Monterrey, Av. Batallón de San Patricio 112, Real San Agustín, San Pedro Garza García, Nuevo León 66260, Mexico. olivaresyazmin@gmail.com

Abstract

BACKGROUND

Fibroadenoma (FA) is the most common tumor found in young women, although it can occur in any age group. Ductal carcinoma in situ (DCIS) that is confined in a FA is rare; it is most frequently reported as an incidental finding.

CASE SUMMARY

We report a case of DCIS within a FA in a 46-year-old female without cancer-related personal and family histories. The patient was diagnosed with a breast conglomerate of nodules and was followed for 1 year. In the current control image study, we found suspicious microcalcification, as a new finding, within one of the nodules. Consequently, a core biopsy of the tumor, which appeared hypoechoic, oval, and circumscribed, was performed. The pathological diagnosis was ductal carcinoma in situ within a fibroepithelial lesion. The patient underwent breast-conserving surgery and received radiotherapy as well as endocrine therapy (tamoxifen).

CONCLUSION

We recommend a multidisciplinary approach for adequate treatment and follow-up.

Key Words: Carcinoma *in situ*; Fibroadenoma; Mammography; Ultrasound; Magnetic resonance imaging; Radiology; Case report

©The Author(s) 2024. Published by Baishideng Publishing Group Inc. All rights reserved.

Core Tip: Fibroadenoma (FA) is the most common tumor found in women. Although it can occur in any age group, is important to consider when to suspicious a malignant change of FA. The case we report is of great interest to the radiology community because ductal carcinoma in situ within a FA is a challenge to diagnosis. The aim of this case report is to present the current findings in imaging studies for an early diagnosis and to not delay the treatment.

Citation: Olivares-Antúnez Y, Dávila-Zablah YJ, Vázquez-Ávila JR, Gómez-Macías GS, Mireles-Aguilar MT, Garza-Montemayor ML. Ductal carcinoma in situ within a fibroadenoma: A case report and review of literature. *World J Radiol* 2024; 16(3): 58-68
URL: https://www.wjgnet.com/1949-8470/full/v16/i3/58.htm
DOI: https://dx.doi.org/10.4329/wjr.v16.i3.58

INTRODUCTION

Ductal carcinoma in situ (DCIS) arising within a fibroadenoma (FA) is rarely encountered, although pure FA is the most common tumor found. Its incidence ranges from 0.02% to 0.125%, and it is incidentally found. We present a case of breast DCIS arising within a FA and discuss the imaging findings.

CASE PRESENTATION

Chief complaints

The 46-year-old female was diagnosed with a conglomerate of breast nodules which is stable for a period of 1 year. She came to our department for routine mammography and follow-up nodules by ultrasound (US).

History of present illness

She is asymptomatic.

Personal and family history

Family history: Cervical cancer (her mother was diagnosed at age 81 and her sister was diagnosed at age 50). Gastric cancer (her grandmother diagnosed at age 80).

Personal history: The patient had a history of augmentation mammoplasty.

Physical examination

Right breast without palpable mass. Right and left axillary lymph nodes clinically negative.

Imaging examinations

By mammography, the tissue breast is extremely dense (category "D" of the American College of Radiology, 2013). In the right breast, a conglomerate of nodules with obscured margins is seen at the posterior third of the union of lower quadrants. In both axillary regions, no lymph nodes are shown (Figure 1).

Craniocaudal and Mediolateral Oblique projections with magnification of right breast reveal two confluence nodules, which are isodense, oval with obscured margins and microcalcifications associated. The findings are localized 2 cm from skin adjacent to the mastoplasty surgical scar indicated by the linear tissue marker (Figure 2).

In addition, the magnification views in orthogonal projections reveal that one of the nodules is associated with fine and linear pleomorphic microcalcifications that extended in an area of 8 mm (Figure 3).

By digital breast tomosynthesis, we corroborate the morphology of microcalcifications (Figure 4).

Subsequently, a bilateral breast US was performed. In the right breast is seen a conglomerate of two solid nodules that are hypoechoic, oval, circumscribed, avascular and non-palpable, located at the 6 o'clock position, 4 cm from the nipple in the right breast (Figure 5). One of the nodules shows microcalcifications seen in mammography. The bilateral axillary region demonstrates lymph nodes with morphology and fat hilum conservation (Figure 6). These findings correspond to the category of breast imaging-reporting and data system (BI-RADS) 4B.

An US-guided core biopsy was indicated. A percutaneous biopsy was performed of the conglomerate solid nodules, using a 12-gauze needle. Six cores were obtained and sent in formalin for pathology analysis. A tissue marker (or clip) is placed in one of the nodules which is associated with macrocalcifications. A projection of mammography is taken to

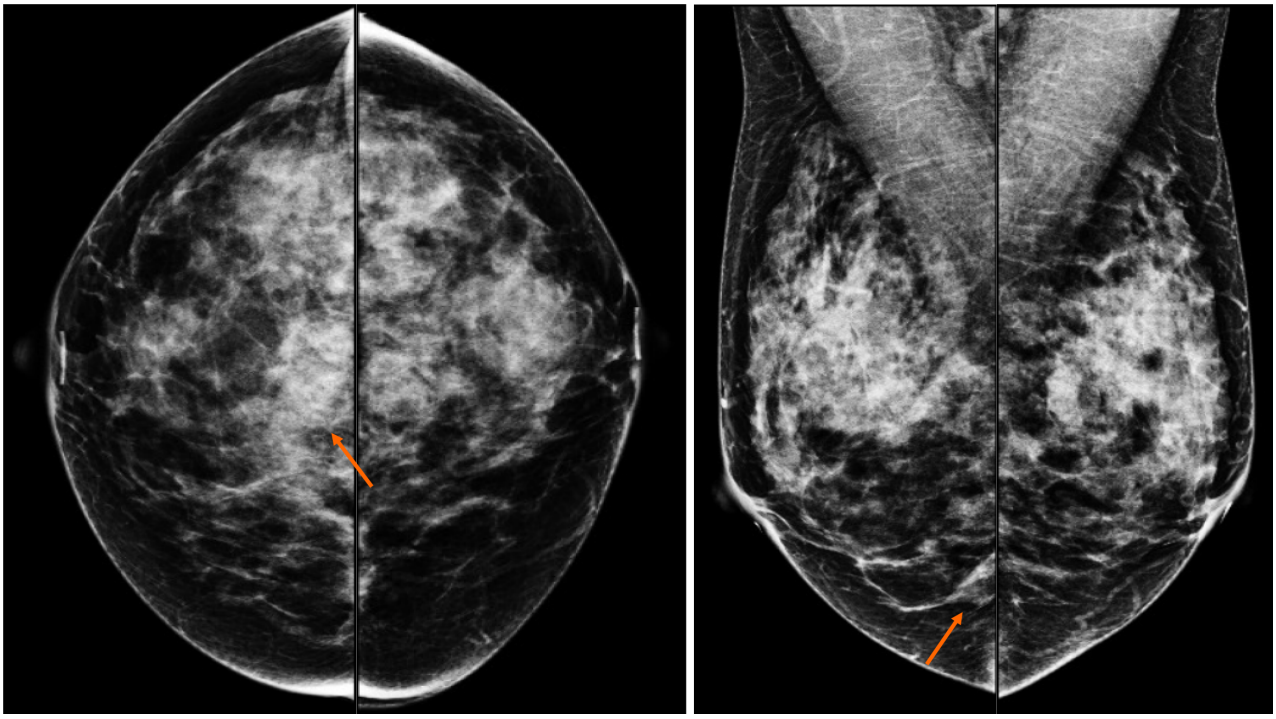

Figure 1 Craneocaudal and Mediolateral Oblique projections of mammography. The breast tissue is extremely dense (category "D" of the American College of Radiology, 2013). In the right breast exists a conglomerate of nodules (arrow) localized at the third posterior of the union of lower quadrants, they are two isodense and oval nodules with obscured margins.

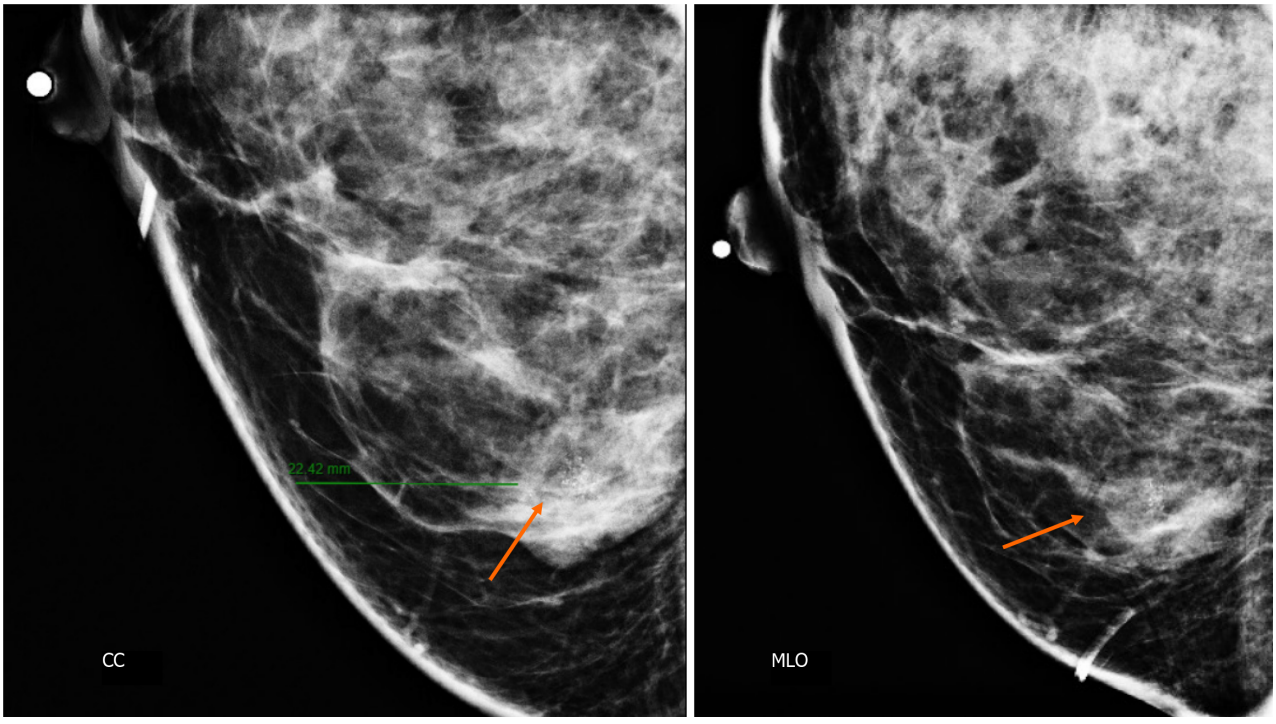

Figure 2 Craniocaudal and mediolateral oblique projections with magnification of right breast. The two confluence nodules are associated with suspicious microcalcifications (arrow). The findings are localized 2 cm from skin and are adjacent to mastoplasty surgical scar indicated by the linear tissue marker as it is seen in the mediolateral oblique projection. CC: Craniocaudal; MLO: Mediolateral oblique.

confirm the position of the tissue marker (Figure 7).

The histopathology report corresponds to 1.5 mm of high–nuclear grade DCIS with comedonecrosis and microcalcifications, which are within a fibroephitelial lesion that corresponds to a FA. Hematoxylin and eosin stain slides revealed pleomorphic neoplastic cells within a FA (Figure 8).

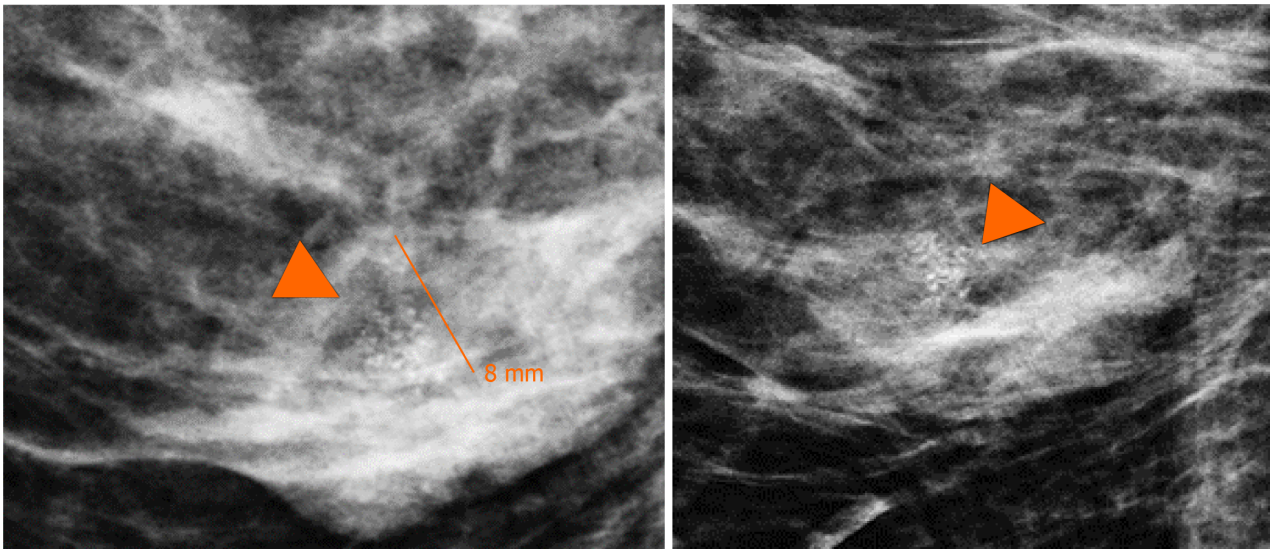

Figure 3 Magnification views in orthogonal projections. One of the nodules is associated with fine and linear pleomorphic microcalcifications (head arrow) that extended in an area of 8 mm.

TREATMENT

The patient underwent surgery, involving guidewire localization of the non-palpable conglomerate of nodules done under US (Figure 9). The treatment consists of conserving surgery and no sentinel lymph node biopsy was needed.

FINAL DIAGNOSIS

The pathological report corresponds to residual tumor of 0.5 mm foci which corresponds to a high–nuclear grade DCIS, comedo subtype, central necrosis and microcalcifications associated within a complex FA, that measures 2.5 cm.

Stage 0, cTisN0M0 within a FA, with the following immunochemistry markers: Estrogen receptor (+) 90% and progesterone receptor (+) 70% (Figure 10).

Other histological findings: Columnar cell changes and hyperplasia with microcalcifications and 2 peripheral papillomas, one measures 0.7 mm.

OUTCOME AND FOLLOW-UP

The patient subsequently received radiotherapy and endocrine therapy (tamoxifen). According to the final diagnosis the patient has a good prognosis.

DISCUSSION

FA is the most common benign fibroepithelial breast tumor in young women and can occur at any age, being most common between 20 years and 40 years of age[1-13].

FA is a biphasic tumor composed of stromal (connective) and epithelial tissue that grows by estrogen and progesterone stimulation and is commonly found in pregnancy and lactation. During menopause, FAs suffer atrophy[3,4,6,9,13].

FAs are divided into simple and complex types. FAs with 1 or more of the following characteristics are considered complex: Epithelial calcifications, apocrine metaplasia, sclerosing adenosis and/or cysts larger than 3 mm[1,4-7,9,11,12,14].

The risk of breast carcinoma in complex FAs is 3.10 times greater than in patients with pure FAs and is associated with the percentage of epithelial proliferation[1,3,5,13].

DCIS within a breast FA is uncommon, with an incidence of 0.02% to 0.125%. Fewer than 130 cases have been reported in the literature[1].

Cancer may arise from the surrounding breast tissue, in the fissures of the FA, or the carcinoma may be completely confined within the FA. The age at presentation of these patients is 42.5 to 46.9 years-old, approximately 20 years later than the maximum age at presentation of patients with pure FA[1,6,10,12].

There are no specific imaging characteristics to distinguish between a pure FA and DCIS within a FA. In most cases, DCIS presents as an incidental finding and is indistinguishable from benign lesions on imaging (Table 1)[1].

Table 1 Differential diagnosis microcalcifications within a nodule

Diagnosis	Description of microcalcifications
Ductal carcinoma in situ within fibroadenoma	Fine or linear pleomorphic
Fat necrosis	Coarse calcifications and round or curvilinear calcifications in cyst wall
Initial degenerating fibroadenoma	Numerous, dense and peripherical located in a nodule and the coarse pathognomonic calcifications
Benign or malignant phyllodes tumor	Coarse, amorphous, and punctuate
Phyllodes tumor with carcinoma component	Benign-looking specks or suspicious coarse punctate
Triple-negative tumor	Clustered microcalcifications
Mucinous carcinoma	Round, coarse, amorphous and/or rarely pleomorphic
Papillary carcinoma	Pleomorphic, coarse, or stippled
Metaplastic carcinoma	Amorphous, fine pleomorphic, fine linear, and lastly coarse heterogeneous

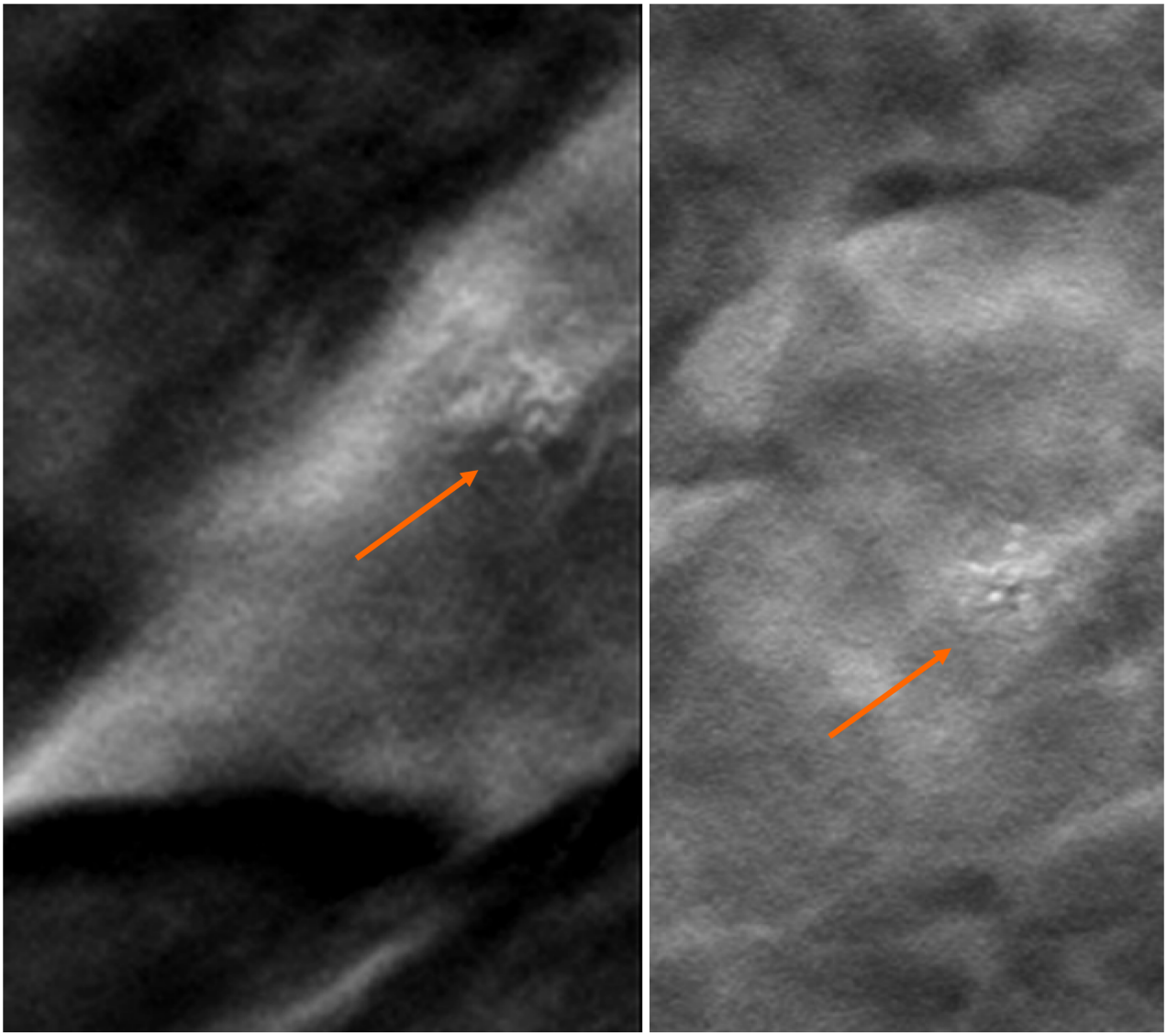

Figure 4 Digital breast tomosynthesis with magnification of craniocaudal and mediolateral oblique projections. The morphology of microcalcifications is corroborated as fine and linear pleomorphic appearance (arrow).

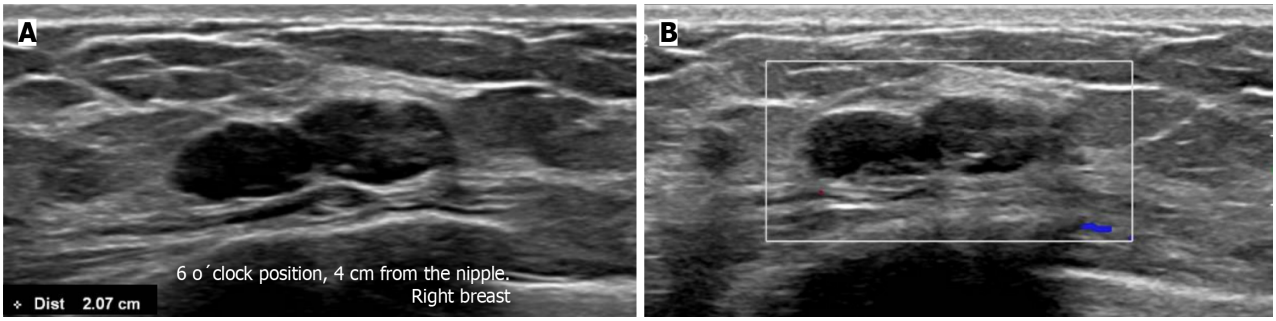

Figure 5 Gray-scale ultrasound and Doppler color images. A: In the right breast is seen a conglomerate of two solid nodules that are hypoechoic, oval, circumscribed and non-palpable with lateral acoustic shadowing, located at the 6 o'clock position, 4 cm from the nipple in the right breast. In one of the nodules, internal hyperechoic foci are seen, corresponding to microcalcifications shown in mammography; B: The nodules have neither internal nor peripherical vascularity.

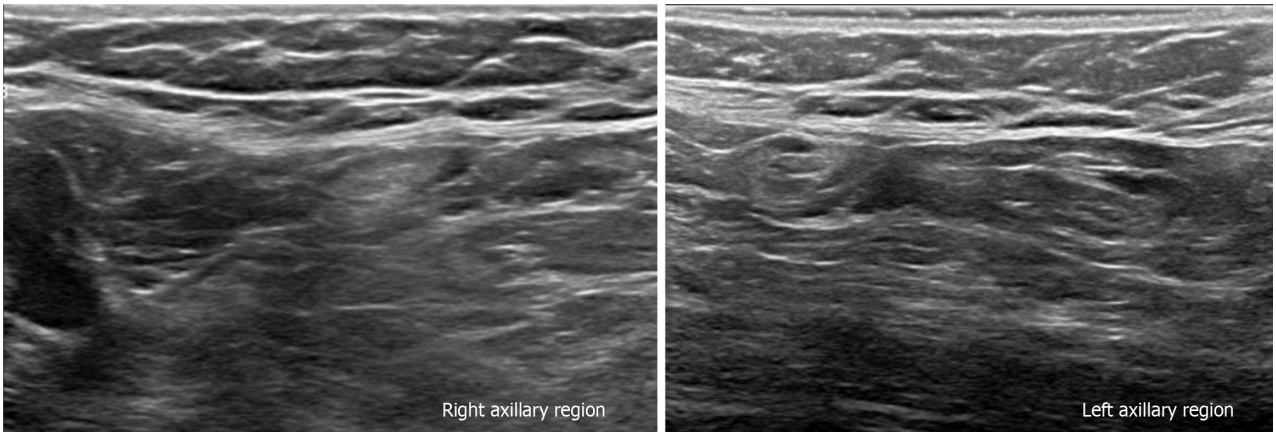

Figure 6 Gray-scale ultrasound images. The bilateral axillary region shows lymph nodes with conservative morphology and fat hilum, with cortex of < 3 mm.

The suspicious finding of carcinoma in a FA in mammography is a group of fine or linear pleomorphic microcalcifications within a nodule of indistinct margins[1-4,6,7,9,12,14].

By US, if the shape or margin of the nodule is irregular and has acoustic shadowing, an echogenic halo or distortion of the architecture should be considered suspicious for malignancy[1-4,6,7].

By magnetic resonance imaging (MRI), a typical FA is observed as an oval mass, with circumscribed margins and persistent contrast enhancement. A carcinoma should be suspected when there is contrast enhancement with a rapid uptake curve and washout late phase (type 3)[1,3,6,7].

In adult patients, the American Society of Breast Surgeons recommends against routinely excising biopsy-proven FA that are < 2 cm. The American College of Radiology Appropriateness Criteria for palpable breast masses even states that short term imaging follow-up (such as every 6 months for 2 years) is a reasonable alternative to biopsy for solid masses with probably benign features suggesting FA[15].

A core biopsy should be performed on a nodule that presents rapid growth. The criteria for rapid growth are: (1) Volume growth rate ≥ 16% per month for patients younger than 50 years; (2) volume growth ≥ 13% per month for patients ≥ 50 years; and (3) mean change in dimension over a 6-month interval of > 20, especially in patients over 40 years of age to exclude the possibility of phyllodes tumor or malignancy[15].

The indications for excision include size > 30 mm, considering that pre-operative biopsy is also insufficient to distinguish phyllodes tumor from FA, and there is the possibility of underestimation. Other indications for surgical removal are for growing FA, a nodule with increased BI-RADS classification grade during the follow-up and core needle biopsy suggesting atypical hyperplasia or unusual pathologic features. Persistent discomfort and pain from a FA are a relative indication to consider surgical excision. Another indication for surgical removal is patient´s request or cosmetic concerns[6,16-19].

The differential diagnoses to consider for a nodule with suspicious microcalcifications are fat necrosis, initial degenerating FA, phyllodes tumor, triple-negative, mucinous, papillary, and metaplastic carcinoma (Table 1)[6,20].

Fat necrosis can be seen as a circumscribed soft-tissue mass with or without macro- or microcalcifications. At mammography, fat necrosis may be characterized by lipid cysts, microcalcifications, coarse calcifications near architectural distortion of surgical scar and focal masses[20,21].

The classic degenerating FA contains coarse pathognomonic calcifications. Occasionally, at the initial period of involution, the calcifications are small, numerous and may have a malignant appearance. Mammography helps to distinguish from ductal carcinoma. The microcalcifications in carcinomas are commonly small and asymmetrically located in a small area, whereas those in FAs tend to be denser, and more diffusely spaced or peripherical located in a

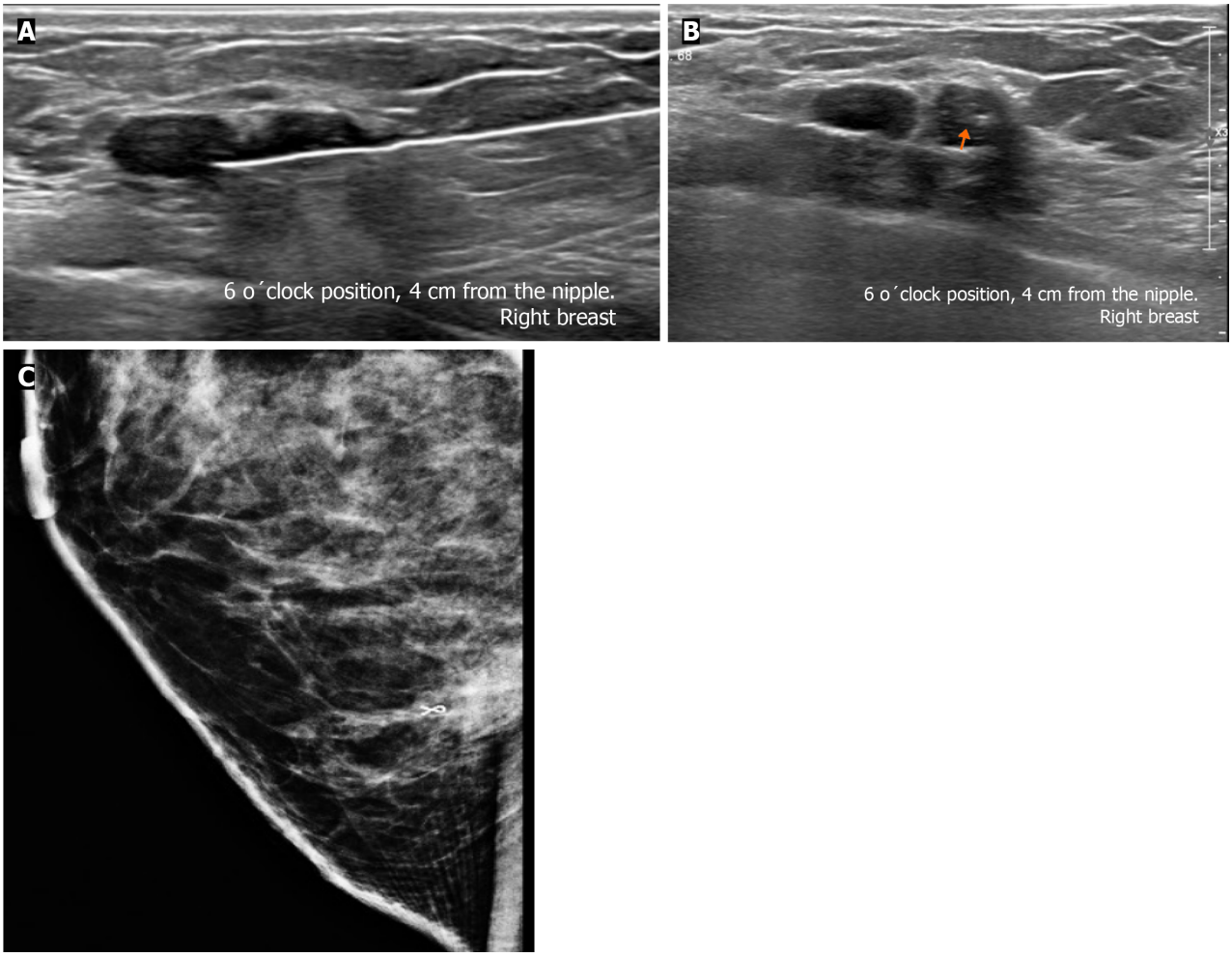

Figure 7 Ultrasound-guided core biopsy images. A: Percutaneous biopsy was performed of the conglomerate solid nodules, using a 12-gauze needle; B: A tissue marker or clip is placed in one of the nodules (arrow) which is associated with microcalcifications; C: Lateral projection of mammography. The tissue marker confirms the position of biopsied microcalcifications.

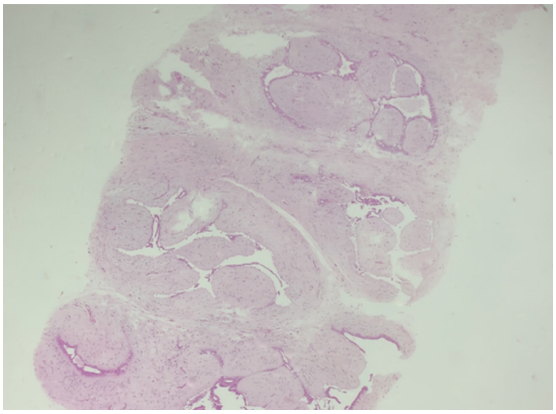

Figure 8 Hematoxylin and eosin stain slide. Pleomorphic neoplastic cells are seen within a fibroadenoma.

nodule[20].

The phyllodes tumor is observed as a dense, round, or oval mass with circumscribed or indistinct margins. Liberman *et al*[22]. described 4 cases of benign and malignant phyllodes tumors containing coarse, amorphous, and punctuate microcalcifications. Also, the presence of benign-looking specks or suspicious coarse punctate clusters of microcalcifications is reported in less than a third (29%) of phyllodes tumors with a carcinoma component, which would significantly change the subsequent management plan. By US the phyllodes tumor is round or oval, heterogeneous with cystic areas and posterior acoustic enhancement. By MRI, it is a round, lobulated mass with circumscribed margins. When the tumor presents cystic areas, the mass is hypointense on T1-sequences and hyperintense on T2-sequences. Only 33% of these

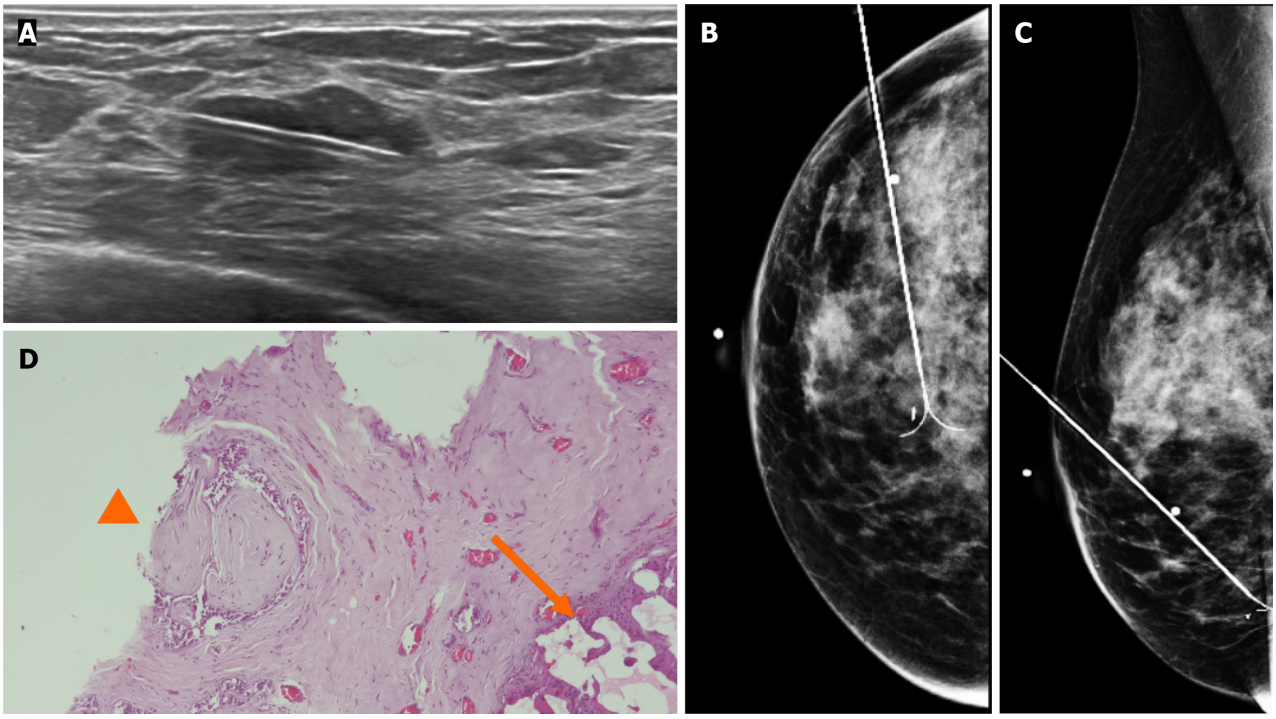

Figure 9 Gray-scale ultrasound images. A: Preoperative guidewire is inserted percutaneously into the breast to localize the non-palpable conglomerate of nodules done under ultrasound; B and C: Craniocaudal and mediolateral oblique projection. The adequate position of the hook wire is confirmed in the target lesion; D: Histological slide of partial mastectomy. The site of the previous biopsy is seen (arrow). Also, fibroadenoma is shown which contains pleomorphic neoplastic cells and nucleolus with pleomorphic appearance (head arrow) that corresponds to ductal carcinoma in situ.

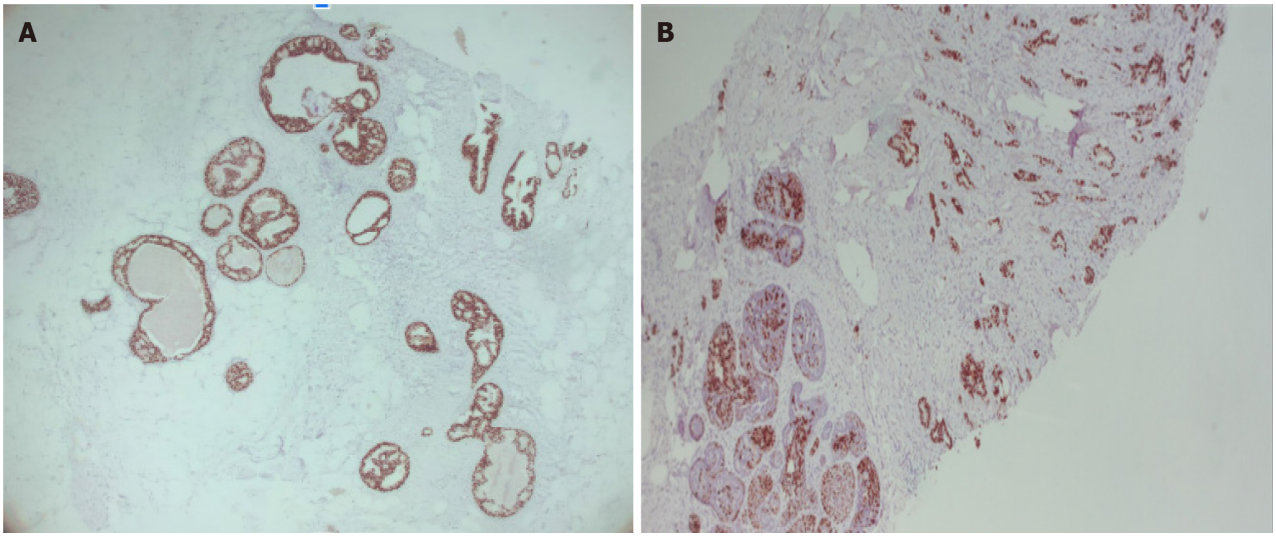

Figure 10 Immunohistochemical staining. A: Immunohistochemical markers 5 ×, estrogen receptor + (90%) in ductal carcinoma in situ within fibroadenoma; B: Immunohistochemical markers 5 ×, progesterone receptor (+) 70% in ductal carcinoma in situ within fibroadenoma.

tumors show enhancement, including the internal septa[6,22,23].

Mucinous carcinoma occurs more frequently in older people, and the average age at presentation is 71 years. It represents 1% to 4% of all breast cancers. On mammography, mucinous carcinoma appears as a circumscribed, round, or oval mass of low density, which may resemble a cyst or FA. Microcalcifications are rare, but when are present, they appear as round, coarse, amorphous and/or rarely pleomorphic. Microcalcifications most commonly occur in those tumors that demonstrate papillary or comedo growth patterns. Psammornatous microcalcifications that are seen with other types of mucin-producing tumors have been found in some cases. US shows a round or oval, circumscribed, and isoechoic mass with posterior acoustic enhancement. MRI demonstrates a circumscribed, oval mass, hyperintense on T2 and with heterogeneous enhancement[6,20,24].

The intraductal papillary neoplasms of the breast include papilloma, papilloma with atypical ductal hyperplasia (ADH) or DCIS, papillary DCIS (pDCIS), encapsulated papillary carcinoma (EPC), solid papillary carcinoma (SPC) and

invasive papillary carcinoma (IPC). Papilloma, papilloma with ADH, DCIS, and pDCIS are associated with microcalcification. Papillary carcinomas with microcalcifications within the tumor are usually pleomorphic but may occasionally be coarse or stippled in appearance. US can reveal a hypoechoic solid mass or a complex cyst with septations or mural-based papilliform nodularity. The most common finding of EPC on mammography is a solitary oval or round mass with microlobulated or circumscribed margins and calcifications are not uncommon and are mainly amorphous or pleomorphic. In SPC concomitant microcalcification on mammography was rarely reported in the literature cases and 33.32% were accompanied by amorphous calcifications. Sonographically has been reported as multiple nodules accompanied by ductal ectasia, well-circumscribed, complex, cystic lesion, and homogeneous solid lesions. Ciurea *et al* [25]. reported IPCs as round or lobulated masses, often associated with mammographic calcification. Micropapillary DCIS is frequently associated with "snake skin-like" microcalcification[25-27].

In Krizmanich-Conniff *et al*[28] series found that 7% of triple-negative carcinoma appeared as clustered microcalcifications, whilst another 29% manifested as masses with associated microcalcifications. The rapid growth, with no precancerous stage, also explains the low incidence of microcalcifications. Microcalcifications inside a mass or isolated segmental type calcifications were more often associated with a DCIS and a human epidermal growth factor receptor 2+ status. On US and MRI images, commonly theses tumors appear as a round or oval mass with irregular, spiculated, or circumscribed margins with rapid early enhancement and a late washout curve[6,28,29].

Metaplastic breast cancer, on mammography, are commonly large masses of 4.2 cm, with high density and smooth, well-defined and spiculated margins. Microcalcifications are very rare within the mass; when this happens, they are more likely to be amorphous, fine pleomorphic, fine linear, and lastly coarse heterogeneous[30,31].

It is important to understand that suspicious microcalcifications within masses can indicate the presence of malignancies such as mucinous carcinoma, metaplastic carcinoma with less incidence than CDIS within FA. In our case, microcalcifications have to be distinguished from fat necrosis because their localization is near surgical scar. Is not frequent to encounter CDIS within a nodule but the radiologist has to be aware of it. A stereotactic biopsy may be used to remove the group of microcalcifications however there were at 2 cm from the skin, which contraindicated this interventional procedure. According to the site of the findings in mammography, we corroborated that the microcalcifications that were seen within one of the nodules were the suspicious group, therefore we were able to make the biopsy by US instead of used stereotactic-guided vacuum-assisted system. After the diagnosis of DCIS was reported by pathologist, to assurance a successful surgery for nonpalpable nodule, wire localization is needed. The limitation of our case is that MRI images of this patient are not available in our Institution, and we cannot detail the findings by this method.

The treatment of choice is conservative surgery, if 2 or fewer suspicious lymph nodes are found on imaging, or 2 or fewer positive lymph nodes are confirmed by needle biopsy, then is recommended sentinel lymph node mapping. Adjuvant therapy includes radiotherapy and endocrine therapy. The majority have good prognosis, with no difference between young and older women. Ten percent of patients present with recurrence or metastasis[1-3,6,9].

CONCLUSION

FAs are common in imaging studies, but the presence of a DCIS within the nodule is rare and has nonspecific findings on imaging. Faced with a circumscribed nodule within microcalcifications is a diagnostic challenge and by imaging studies can simulate benign and malignant pathologies. The radiologist has to consider in the differential diagnosis DCIS within a FA or other round tumors associated with microcalcifications, and the core biopsy should be performed. We recommend a multidisciplinary approach for adequate treatment and follow-up.

FOOTNOTES

Author contributions: Olivares-Antúnez Y performed searched the literature and wrote the manuscript; Dávila-Zablah YJ performed the research and reviewed the manuscript; Vázquez-Ávila JR and Gómez-Macías GS performed the subtraction image processing, discussed the results and contributed to the final manuscript; Mireles-Aguilar MT was the primary surgeon, and provided surgical insights into the case; and Garza-Montemayor ML was the senior author who supervised and made substantial contributions to the conception of the work.

Informed consent statement: Informed written consent was obtained from the patient for the publication of this report and any accompanying images.

Conflict-of-interest statement: All the authors report no conflicts of interest for this article.

CARE Checklist (2016) statement: The authors have read the CARE Checklist (2016), and the manuscript was prepared and revised according to the CARE Checklist (2016).

Open-Access: This article is an open-access article that was selected by an in-house editor and fully peer-reviewed by external reviewers. It is distributed in accordance with the Creative Commons Attribution NonCommercial (CC BY-NC 4.0) license, which permits others to distribute, remix, adapt, build upon this work non-commercially, and license their derivative works on different terms, provided the original work is properly cited and the use is non-commercial. See: https://creativecommons.org/Licenses/by-nc/4.0/

Country/Territory of origin: Mexico

ORCID number: Yazmin Olivares-Antúnez 0000-0002-3588-645X; Yesika Janett Dávila-Zablah 0000-0002-5153-2360; José Raúl Vázquez-Ávila 0009-0004-4592-5899; Gabriela Sofía Gómez-Macías 0000-0003-4849-492X.

S-Editor: Luo ML
L-Editor: A
P-Editor: Zhao S

REFERENCES

1 **Ni XH**, An R, Shi QW, Wang CL. Low-Grade Ductal Carcinoma in situ Within a Fibroadenoma of the Breast: A Rare Case Report and Review of the Literature. *Onco Targets Ther* 2023; **16**: 399-406 [PMID: 37325202 DOI: 10.2147/OTT.S413223]
2 **Wu J**, Sun KW, Mo QP, Yang ZR, Chen Y, Zhong MC. Preoperational diagnosis and management of breast ductal carcinoma in situ arising within fibroadenoma: Two case reports. *World J Clin Cases* 2022; **10**: 3496-3504 [PMID: 35611194 DOI: 10.12998/wjcc.v10.i11.3496]
3 **Hammood ZD**, Mohammed SH, Abdulla BA, Omar SS, Naqar S, Salih AM, Kakamad FH. Ductal carcinoma in situ arising from fibroadenoma; a rare case with review of literature. *Ann Med Surg (Lond)* 2022; **75**: 103449 [PMID: 35386780 DOI: 10.1016/j.amsu.2022.103449]
4 **Brunetti N**, Valente I, Pitto F, Calabrese M. Triple-negative Breast Cancer Arising in a Fibroadenoma in BRCA 1 Mutated Patient. *J Med Ultrasound* 2023; **31**: 63-65 [PMID: 37180614 DOI: 10.4103/jmu.jmu_83_21]
5 **Shojaku H**, Hori R, Yoshida T, Matsui K, Shimada K, Takayanagi N, Noguchi K. Low-grade ductal carcinoma in situ (DCIS) arising in a fibroadenoma of the breast during 5 years follow-up: A case report. *Medicine (Baltimore)* 2021; **100**: e24023 [PMID: 33725814 DOI: 10.1097/MD.0000000000024023]
6 **Feliciano YZ**, Freire R, Net J, Yepes M. Ductal and lobular carcinoma in situ arising within an enlarging biopsy proven fibroadenoma. *BMJ Case Rep* 2021; **14** [PMID: 33468635 DOI: 10.1136/bcr-2020-237017]
7 **Kato F**, Omatsu T, Matsumura W, Takahashi M, Hosoda M, Takahashi H, Kubota K, Oyama-Manabe N, Terae S, Shirato H. Dynamic MR findings of ductal carcinoma in situ within a fibroadenoma. *Magn Reson Med Sci* 2011; **10**: 129-132 [PMID: 21720115 DOI: 10.2463/mrms.10.129]
8 **Fukuda M**, Nagao K, Nishimura R, Matsuda M, Baba K, Ueno Y, Morinaga H, Omachi H, Hamada T. Carcinoma arising in fibroadenoma of the breast--a case report and review of the literature. *Jpn J Surg* 1989; **19**: 593-596 [PMID: 2593394 DOI: 10.1007/BF02471669]
9 **El-Essawy M**, AL Haidary A, Khan AL. Ductal carcinoma in situ (DCIS) in breast fibroadenoma. *Egypt J Radiol Nucl Med 51* 2020; **73** [DOI: 10.1186/s43055-020-00191-5]
10 **Ren Y**, Li P, Yang Y, Huang Y, Zhan D, Wen B. Imaging findings of ductal carcinoma in situ arising within fibroadenoma. *Breast J* 2020; **26**: 1037-1038 [PMID: 31837072 DOI: 10.1111/tbj.13709]
11 **Fujimoto A**, Matsuura K, Kawasaki T, Ichinose Y, Nukui A, Hiratsuka M, Asano A, Shimada H, Osaki A, Saeki T. Early HER2-positive breast cancer arising from a fibroadenoma: a case report. *Oxf Med Case Reports* 2021; **2021**: omab083 [PMID: 34527256 DOI: 10.1093/omcr/omab083]
12 **Borecky N**, Rickard M. Preoperative diagnosis of carcinoma within fibroadenoma on screening mammograms. *J Med Imaging Radiat Oncol* 2008; **52**: 64-67 [PMID: 18373829 DOI: 10.1111/j.1440-1673.2007.01913.x]
13 **Dupont WD**, Page DL, Parl FF, Vnencak-Jones CL, Plummer WD Jr, Rados MS, Schuyler PA. Long-term risk of breast cancer in women with fibroadenoma. *N Engl J Med* 1994; **331**: 10-15 [PMID: 8202095 DOI: 10.1056/nejm199407073310103]
14 **Baker KS**, Monsees BS, Diaz NM, Destouet JM, McDivitt RW. Carcinoma within fibroadenomas: mammographic features. *Radiology* 1990; **176**: 371-374 [PMID: 2164233 DOI: 10.1148/radiology.176.2.2164233]
15 **Harvey JA**, Mahoney MC, Newell MS, Bailey L, Barke LD, D'Orsi C, Hayes MK, Jokich PM, Lee SJ, Lehman CD, Mainiero MB, Mankoff DA, Patel SB, Reynolds HE, Sutherland ML, Haffty BG. ACR Appropriateness Criteria Palpable Breast Masses. *J Am Coll Radiol* 2016; **13**: e31-e42 [PMID: 27814822 DOI: 10.1016/j.jacr.2016.09.022]
16 **Sklair-Levy M**, Sella T, Alweiss T, Craciun I, Libson E, Mally B. Incidence and management of complex fibroadenomas. *AJR Am J Roentgenol* 2008; **190**: 214-218 [PMID: 18094314 DOI: 10.2214/AJR.07.2330]
17 **Peng Y**, Xie F, Zhao Y, Wang S; Chinese Society of Breast Surgery. Clinical practice guideline for breast fibroadenoma: Chinese Society of Breast Surgery (CSBrS) practice guideline 2021. *Chin Med J (Engl)* 2021; **134**: 1014-1016 [DOI: 10.1097/CM9.0000000000001462]
18 **Kopkash K**, Yao K. The surgeon's guide to fibroadenomas. *Ann Breast Surg* 2020; **4**: 25-25 [DOI: 10.21037/abs-20-100]
19 **Gillette DP**, He J, Lee AE, Chao C. Indications for the surgical excision of fibroadenomas: systematic review. *AME Surg J* 2023; **3**: 3 [DOI: 10.21037/asj-21-87]
20 **Ranveer SA**, Biren AS, Dongping S. Mucinous Carcinoma of the breast: Mammography and Ultrasound Appearance with Histopathology Correlation. *JOJ Case Stud* 2019; **9**: 555774 [DOI: 10.19080/jojcs.2019.09.555774]
21 **Kerridge WD**, Kryvenko ON, Thompson A, Shah BA. Fat Necrosis of the Breast: A Pictorial Review of the Mammographic, Ultrasound, CT, and MRI Findings with Histopathologic Correlation. *Radiol Res Pract* 2015; **2015**: 613139 [PMID: 25861475 DOI: 10.1155/2015/613139]
22 **Liberman L**, Bonaccio E, Hamele-Bena D, Abramson AF, Cohen MA, Dershaw DD. Benign and malignant phyllodes tumors: mammographic and sonographic findings. *Radiology* 1996; **198**: 121-124 [PMID: 8539362 DOI: 10.1148/radiology.198.1.8539362]
23 **Yuen WN**, Li JJX, Chan MY, Tse GM. High-grade ductal carcinoma in-situ detected by microcalcification within borderline phyllodes tumor: Report of a case and literature review. *Hum Pathol Repo* 2023; **31**: 300697 [DOI: 10.1016/j.hpr.2023.300697]
24 **Shin GW**, Park HY, Park YM. Mucinous Breast Carcinoma Presenting as a Coarse and Densely Calcified Mass on Mammography: A Case Report. *Taehan Yongsang Uihakhoe Chi* 2020; **81**: 1266-1271 [PMID: 36238037 DOI: 10.3348/jksr.2019.0083]
25 **Ciurea A**, Calin A, Ciortea C, Dudea SM. Ultrasound in the diagnosis of papillary breast lesions. *Med Ultrason* 2015; **17**: 392-397 [PMID: 26343090 DOI: 10.11152/mu.2013.2066.173.aci]
26 **Kurtoğlu Özçağlayan Tİ**, Öznur M. Digital Mammography, Ultrasound and Magnetic Resonance Imaging Characteristics in Differential Diagnosis of Papillary Carcinoma Subtypes of the Breast and Diagnostic Challenges. *Eur J Breast Health* 2022; **18**: 172-181 [PMID: 35445176 DOI: 10.4274/ejbh.galenos.2022.2021-9-4]

27 **Kulka J**, Madaras L, Floris G, Lax SF. Papillary lesions of the breast. *Virchows Arch* 2022; **480**: 65-84 [PMID: 34734332 DOI: 10.1007/s00428-021-03182-7]
28 **Krizmanich-Conniff KM**, Paramagul C, Patterson SK, Helvie MA, Roubidoux MA, Myles JD, Jiang K, Sabel M. Triple receptor-negative breast cancer: imaging and clinical characteristics. *AJR Am J Roentgenol* 2012; **199**: 458-464 [PMID: 22826413 DOI: 10.2214/AJR.10.6096]
29 **Boisserie-Lacroix M**, Mac Grogan G, Debled M, Ferron S, Asad-Syed M, Brouste V, Mathoulin-Pelissier S, Hurtevent-Labrot G. Radiological features of triple-negative breast cancers (73 cases). *Diagn Interv Imaging* 2012; **93**: 183-190 [PMID: 22421282 DOI: 10.1016/j.diii.2012.01.006]
30 **Corso G**, Criscitiello C, Nicosia L, Pesapane F, Vicini E, Magnoni F, Sibilio A, Zanzottera C, De Scalzi AM, Mannucci S, Marabelli M, Calvello M, Feroce I, Zagami P, Porta FM, Toesca A, Tarantino P, Nicolò E, Mazzarol G, La Vecchia C, Bonanni B, Leonardi MC, Veronesi P, Fusco N. Metaplastic breast cancer: an all-round multidisciplinary consensus. *Eur J Cancer Prev* 2023; **32**: 348-363 [PMID: 37021548 DOI: 10.1097/CEJ.0000000000000794]
31 **Asare B**, White MJ, Rossi J. Metaplastic carcinoma with osteosarcomatous differentiation in the breast: Case report. *Radiol Case Rep* 2023; **18**: 4272-4280 [PMID: 37771380 DOI: 10.1016/j.radcr.2023.08.101]

World Journal of Radiology

Submit a Manuscript: https://www.f6publishing.com

World J Radiol 2024 March 28; 16(3): 69-71

DOI: 10.4329/wjr.v16.i3.69

ISSN 1949-8470 (online)

LETTER TO THE EDITOR

Artificial intelligence for disease diagnostics still has a long way to go

Jian-She Yang, Qiang Wang, Zhong-Wei Lv

Specialty type: Computer science, artificial intelligence

Provenance and peer review: Unsolicited article; Externally peer reviewed.

Peer-review model: Single blind

Peer-review report's scientific quality classification

Grade A (Excellent): 0
Grade B (Very good): B
Grade C (Good): 0
Grade D (Fair): 0
Grade E (Poor): 0

P-Reviewer: Alsamhi SH, Ireland

Received: January 4, 2024
Peer-review started: January 4, 2024
First decision: March 2, 2024
Revised: March 6, 2024
Accepted: March 14, 2024
Article in press: March 14, 2024
Published online: March 28, 2024

Jian-She Yang, Department of Nuclear Medicine, Shanghai Tenth People's Hospital, Tongji University School of Medicine, Shanghai 200072, China

Jian-She Yang, Qiang Wang, Basic Medicine College, Gansu Medical College, Pingliang 744000, Gansu Province, China

Zhong-Wei Lv, Department of Nuclear Medicine, Shanghai Tenth People's Hospital of Nanjing Medical University, Shanghai 200072, China

Corresponding author: Jian-She Yang, MD, MSc, PhD, Academic Editor, Academic Fellow, Chairman, Chief Technician, Dean, Full Professor, Shanghai Tenth People's Hospital, Tongji University School of Medicine, No. 301 Yanchang Road (M), Shanghai 200072, China. 2305499@tongji.edu.cn

Abstract

Artificial intelligence (AI) can sometimes resolve difficulties that other advanced technologies and humans cannot. In medical diagnostics, AI has the advantage of processing figure recognition, especially for images with similar characteristics that are difficult to distinguish with the naked eye. However, the mechanisms of this advanced technique should be well-addressed to elucidate clinical issues. In this letter, regarding an original study presented by Takayama *et al*, we suggest that the authors should effectively illustrate the mechanism and detailed procedure that artificial intelligence techniques processing the acquired images, including the recognition of non-obvious difference between the normal parts and pathological ones, which were impossible to be distinguished by naked eyes, such as the basic constitutional elements of pixels and grayscale, special molecules or even some metal ions which involved into the diseases occurrence.

Key Words: Artificial intelligence; Figure recognition; Diagnosis; AI interactive mechanisms

©The Author(s) 2024. Published by Baishideng Publishing Group Inc. All rights reserved.

Core Tip: We strengthened the importance of mechanism elucidation of the advanced artificial intelligence in processing figures recognition, especially for those images with very similar characteristics that are difficult to be distinguished by the naked eye, and expressed a caution on decision making by using artificial intelligence technique for medical use, in that the unidentified potential would result in a bias.

Citation: Yang JS, Wang Q, Lv ZW. Artificial intelligence for disease diagnostics still has a long way to go. *World J Radiol* 2024; 16(3): 69-71
URL: https://www.wjgnet.com/1949-8470/full/v16/i3/69.htm
DOI: https://dx.doi.org/10.4329/wjr.v16.i3.69

TO THE EDITOR

Recently, Takayama *et al*[1] reported that a branch of artificial intelligence (AI), namely, deep learning (DL), combined with reduced-field-of-view (reduced-FOV) diffusion-weighted imaging, which was identified as field-of-view optimized and constrained undistorted single-shot, has greatly improved image quality without prolonging the scan time for pancreatic cystic lesion diagnostics.

This is an very interested work related the current hot-topic, while, due to the technical shortages, further investigation need to be done during the near future. In terms of these issues, the authors haven't outlined and addressed it in this work rationally. Here we presented some of shortcomings.

In this work, authors have applied the artificial intelligence to distinguish the images for identified diagnosis of pancreatic disease from other related or concurrent diseases, they should also analyze all types of pancreatic images by this technique as systematically as possible. Given the variety of diseases, even the physiological status of pancreatic disease can present diverse physical and chemical characteristics, which are the bases on which AI operates. However, by simply applying the commercial AIR™ Recon DL algorithm (GE Healthcare), the authors have not provided readers the essential and enough information which mentioned above, even in the form of a supplementary material. A complete work should describe the phenomenon with its potential mechanism. Though the AI basic procedures and regulations have been well established by scientists, this interactive episode was absent in this study.

AI can sometimes resolve difficulties that other advanced technologies and humans cannot[2,3]. The authors should effectively illustrate the mechanism and detailed procedure that artificial intelligence techniques processing the acquired images, including the recognition of non-obvious difference between the normal parts and pathological ones of pancreatic, which were not sensitive to naked eyes, such as the pixels and grayscale, special molecules or even some metal ions which involved into the diseases occurrence. All of these presentation will facilitate the understanding of AI processing and recognizing similar or confused images. These are the fundamental principles for artificial intelligence applying in medical use.

FOOTNOTES

Author contributions: Yang JS, Wang Q, and Lv ZW designed the research, analyzed the data and wrote the paper.

Supported by the Dean Responsible Project of Gansu Medical College, No. GY-2023FZZ01; University Teachers Innovation Fund Project of Gansu Province, No. 2023A-182; and Key Research Project of Pingliang Science and Technology, No. PL-STK-2021A-004.

Conflict-of-interest statement: All authors declare that the research was conducted in the absence of any commercial or financial relationships that could be construed as a potential conflict of interest.

Open-Access: This article is an open-access article that was selected by an in-house editor and fully peer-reviewed by external reviewers. It is distributed in accordance with the Creative Commons Attribution NonCommercial (CC BY-NC 4.0) license, which permits others to distribute, remix, adapt, build upon this work non-commercially, and license their derivative works on different terms, provided the original work is properly cited and the use is non-commercial. See: https://creativecommons.org/Licenses/by-nc/4.0/

Country/Territory of origin: China

ORCID number: Jian-She Yang 0000-0001-7069-6072; Qiang Wang 0000-0002-9855-6730; Zhong-Wei Lv 0000-0003-3370-5560.

S-Editor: Liu JH
L-Editor: A
P-Editor: Zhao S

REFERENCES

1 **Takayama Y**, Sato K, Tanaka S, Murayama R, Goto N, Yoshimitsu K. Deep learning-based magnetic resonance imaging reconstruction for improving the image quality of reduced-field-of-view diffusion-weighted imaging of the pancreas. *World J Radiol* 2023; **15**: 338-349 [PMID: 38179202 DOI: 10.4329/wjr.v15.i12.338]

2 **Sahu HK**, Kumar S, Alsamhi SH, Chaube MK, Curry E. Novel Framework for Alzheimer Early Diagnosis using Inductive Transfer Learning Techniques. Proceedings of the 2nd International Conference on Emerging Smart Technologies and Applications (eSmarTA); 2022 Oct 25-26; Ibb, Yemen. United States: IEEE, 2022: 1-7

3 **Kumar S**, Chaube MK, Alsamhi SH, Gupta SK, Guizani M, Gravina R, Fortino G. A novel multimodal fusion framework for early diagnosis and accurate classification of COVID-19 patients using X-ray images and speech signal processing techniques. *Comput Methods Programs Biomed* 2022; **226**: 107109 [PMID: 36174422 DOI: 10.1016/j.cmpb.2022.107109]

Published by **Baishideng Publishing Group Inc**
7041 Koll Center Parkway, Suite 160, Pleasanton, CA 94566, USA
Telephone: +1-925-3991568
E-mail: office@baishideng.com
Help Desk: https://www.f6publishing.com/helpdesk
https://www.wjgnet.com

© 2024 Baishideng Publishing Group Inc. All rights reserved.